LEBANESE AMERICAN UNIVERSITY

Seismic Performance of Slender Concrete Shear Walls with and

without Carbon Fiber Reinforced Polymers Laminates

By

Joanna Youssef Youssef

A thesis submitted in partial fulfillment of the requirements

For the degree of Master of Science in Civil and Environmental Engineering

School of Engineering

December 2022

LAU
الجامعة اللبنانية الأميركية
Lebanese American University

THESIS APPROVAL FORM

Student Name: **Joanna Youssef** I.D. #: 201401016

Thesis Title : Seismic Performance of Slender Concrete Shear Walls with and without Carbon Fiber Reinforced Polymers Laminates

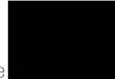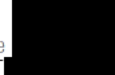Program: Master of science in Civil and Environmental Engineering

Department: Civil Engineering

School: Engineering

The undersigned certify that they have examined the final electronic copy of this thesis and approved it in Partial Fulfillment of the requirements for the degree of:

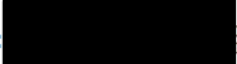Master of science   in the major of   Civil and Environmental Engineering

	Signature		DATE:	Day	Month	Year
Thesis Advisor's Name **Caesar Abi Shdid**	Signature	Digitally signed by Caesar Abi Shdid Date: 2023.01.24 1:03:47 +02'00'	DATE:	24	01	2023
Committee Member's Name **Mazen Tabbara**	Signature	Digitally signed by Mazen Tabbara ...Mazen Tabbara, ou-LAU, Civil Engineering, ...tabbara@lau.edu.lb, ou-LB ...2023.01.26 10:44:22 +02'00'	DATE:	26	01	2023
Committee Member's Name **Wassim Ghannoum**	Signature	Digitally signed by ...ssim M Ghannoum ...: 2023.01.26 ...8:27 -06'00'	DATE:	27	01	2023

ii

LAU

الجامعة اللبنانية الأميركية
Lebanese American University

PLAGIARISM POLICY COMPLIANCE STATEMENT

I certify that:

- I have read and understood LAU's Plagiarism Policy.
- I understand that failure to comply with this Policy can lead to academic and disciplinary actions against me.
- This work is substantially my own, and to the extent that any part of this work is not my own I have indicated that by acknowledging its sources.

Name: Joanna Youssef

Signature ███████████ Digitally signed by joanna youssef
Date: 2022.12.22 13:17:21 +02'00'

Date: 22/12/2022

Dedication

To my beloved family

ACKNOWLEDGMENTS

Seismic Performance of Slender Concrete Shear Walls with and
without Carbon Fiber Reinforced Polymers Laminates

Joanna Youssef Youssef

ABSTRACT

Shear walls are the main lateral-load-resisting system in reinforced concrete buildings. This study examines the seismic performance of slender, under-reinforced shear walls, and proposes retrofit guidelines to enhance the strength and ductility of this type of wall using carbon fiber-reinforced polymer. The in-plane loading performance of the shear wall specimens was examined before and after the retrofit. Two full-scale shear walls were designed and constructed to simulate shear walls in old buildings in the Beirut, Lebanon area. One of the walls was designated to be a control wall and tested as is, while the other was retrofitted using CFRP laminates. The CFRP layout was designed to provide the missing confinement which is usually supplied by special boundary elements configuration present in buildings designed according to modern ACI specifications. The two walls were tested under reversed cyclic loading using a hydraulic actuator. Force deformation plots were produced for both tests and further specific in-plane and out-of-plane displacements were monitored using two high-performance cameras connected to a data acquisition software. Strain gauges were placed at different levels on the wall rebar to monitor their strain profile and yielding points. The study showed that the retrofitted wall had better performance than the control one. Drift capacity was improved by 17% and longitudinal bar buckling was prevented. Moreover, it was observed that the control wall compression zone was completely crushed at 2.5% drift; whereas, the retrofitted wall reached a drift of 3% with an intact concrete section. The CFRP laminates showed to

preserve the concrete core and prevent the buckling of the longitudinal steel bars during cyclic loading. The results of this study will aid in the development of a unified retrofit scheme to enhance the seismic performance of shear walls in old buildings, thus improving their safety in case of a seismic event.

TABLE OF CONTENTS

Chapter   **Page**

LIST OF TABLES

TABLE OF FIGURES

CHAPTER ONE

INTRODUCTION

Given the fact that Lebanon is situated over the Yammoune, Serghaya, and Mount Lebanon faults, it is considered to be a region of high seismic activity. For this reason, proper seismic consideration is vital in the design of structures, especially shear walls which are the main lateral load resisting system. However, most of the buildings especially in the Beirut area were built through the period from the 1960s to the 1990s of the last century. In that period Beirut had a boom in construction due to the displacement of people from the countryside seeking jobs and new lives. As a result, construction was arbitrary and designed only for gravity loads without any consideration for modern seismic design. In these buildings, the shear walls are thin, slender, and lack proper seismic detailing according to recent ACI provisions (minimum wall thickness, minimum reinforcement diameter and layers, special boundary elements). This constitutes a serious threat to over 2.4 million people living in the city in case of a seismic event. Since total replacement of structures has a significant impact on the economy, environment, and resources, the need of implementing maintenance techniques arise, mainly to enhance the ductility, shear strength, and stiffness of a shear wall. According to FEMA (1992), the building flexural can be strengthened by adding additional shear walls, increasing the shear walls' section, or increasing the section reinforcement. These methods will evolve the structure to better resist earthquake loading, but on the other hand, the self-weight of the structure will increase, which will amplify the lateral forces. Moreover, adopting this method can lead

to disruption of the occupancy, and a possible shutdown of the facility during construction. In some cases, these modifications may not be practical or possible. A more advanced process of retrofitting shear walls is the use of carbon fiber-reinforced polymer (CFRP) sheets glued externally to the wall using epoxy according to certain patterns determined by whether the retrofit is used to enhance the shear, flexural, or confinement capacity of members. Numerous studies have addressed the retrofit of structural elements with CFRP laminates. However, the studies concerning shear walls tackled only "short shear walls" which are weak in shear and have a failure mode characterized by the propagation of inclined cracks in the wall section or the separation of the wall from its foundation. This study is one of a two-stage research project that investigates shear walls failure in flexure—a failure mode that is exhibited by out-of-plane buckling and crushing of concrete at the wall toe in the compression region. Experimental data from this study will aid the development of a behavioral model that can be used in the future for the prediction of the responses and failure patterns of similar shear walls. Whereas the second part of this research project proposes new guidelines for retrofit of strength-deficient shear walls in order to improve their performance during seismic events.

CHAPTER TWO

LITERATURE REVIEW

Most of the existing reinforced concrete structures were designed before the development of modern detailing provisions and seismic design codes. The most common failure mechanisms for concrete structures due to seismic loading, according to Dyngeland (1998), are the shear wall failure, the beam to column connection failure, the column failure due to insufficient shear or flexural strength, and the infill wall failure because of the inadequacy of the shear strength or the out-of-plane flexural strength.

Avoiding shear wall failure during seismic events is a significant matter to several researchers because, in many circumstances, the shear walls are the structural elements that provide both lateral force resistance and drift control while simultaneously achieving other functional requirements as stated by Paulay and Priestley (1992).

Design and detailing deficiencies for shear walls, that lack proper seismic detailing according to recent ACI provisions, were reported by several researchers.

In their research, Paterson and Mitchell (2003) studied the core wall of an existing building that had insufficient shear strength required to develop flexural hinging, poor confinement of the boundary elements, inadequate anchorage of the transverse reinforcement, and the presence of lap splices of the longitudinal reinforcement at locations of plastic hinging. Similarly, Layssi et al. (2012) studied shear walls that had the same detailing and design deficiencies of the core wall studied by Paterson and Mitchell

(2003) but had the lap splices of the longitudinal reinforcement present at the base of the wall.

After the Chile 2010 Earthquake, Telleen et al. (2012) reported that most damaged concrete walls suffered from longitudinal bar buckling as well as concrete crushing at the wall base especially at the boundaries. Failure can be caused by the buckling of longitudinal bars due to tensile strains that are followed by compression, or concrete crushing and spalling at the wall base because of the compressive strains. It can also be due to a combination where concrete crushing causes cracking, and then the yielding and buckling of the longitudinal reinforcement leads to crack widening. However, evidence proved that the walls that failed had inadequate transverse reinforcement and bar buckling was reported in all the cases. Besides, walls with well-detailed transverse reinforcement stayed intact, which wouldn't be the case if concrete spalling was the main issue. Thus, bar buckling was the primary cause of damage.

Wallace et al. (2012) also investigated the Chile earthquake, they recorded drift ratios that ranged from 0.8% in 5-story buildings to 1% in buildings having 10 or more stories. Besides, it was found that most of the walls suffered damage concentrated at short heights equal to approximately 1 to 3 times wall thickness due to stress concentrations caused by bar buckling near the wall base. Cyclic strains led to the opening of the used 90-degree hooks which in turn induced bar buckling, the reason for concrete spalling. This greatly affected the wall resistance of thin wall sections where a 2 cm loss of concrete on each side will result in the loss of at least 20% of the wall section.

Rosso et al. (2015) carried out two experimental tests on thin reinforced concrete walls under cyclic loading. The specimens had T-shaped cross-sections and were detailed with

single layers of vertical and horizontal reinforcement in order to simulate the thin walls commonly found in many of Colombia's existing mid- and high-rise low-cost residential structures. The two structural walls had similar dimensions, shear span, reinforcement scheme, and axial load application, but were subjected to different loading patterns: the first wall was subjected to uni-directional loading (in-plane displacements only), while the second wall was subjected to bi-directional loading (in-plane and out-of-plane displacements). Experimental results showed that the two walls experienced large out-of-plane displacements without causing them to have an out-of-plane failure mode; thus, both walls had in-plane failure mode. In addition, the damage induced by these significant out-of-plane deformations caused a strength degradation, which ultimately led the wall to have a premature in-plane failure.

Moreover, slender structural walls have been demonstrated to be vulnerable to lateral instability in previous earthquakes and laboratory testing. To further understand the primary variables that influence instability, an investigation was conducted by several researchers.

Goodsir (1985) conducted a wall testing program in order to assess the observed failure due to out-of-plane instability and the effects of slenderness ratio. He was the first author to perform several tests on thin reinforced concrete structural walls under tension and compression reversed cyclic loading. He examined the lateral stability of slender shear walls subjected to in-plane displacements by idealizing the end-region of the shear wall as an axially loaded reinforced concrete column. Besides, he described in detail the development of the out-of-plane failure mechanism for slender reinforced concrete walls. Finally, it was observed that the potential for the out-of-plane instability of reinforced

concrete units was directly related to the maximum tensile strain reached before consequent compressive loading.

Paulay and Priestley (1993) developed design recommendations to predict the onset of out-of-plane buckling by observing the response while testing rectangular shear walls under severe earthquake loading and by relying on theoretical considerations of structural behavior. Due to the limited availability of experimental evidence, engineering judgment was relied on extensively to attain design recommendations. It was concluded that inelastic buckling was more affected by the length of the wall than by the unsupported height. Besides, the previously experienced inelastic tensile strains of the steel were assumed to be the major sources of the wall instability within the plastic hinge region.

Chai and Elayer (1999) performed an experimental study in order to study the out-of-plane stability of slender reinforced concrete columns reinforced with two layers of vertical bars under large strain amplitude tension/compression load cycles. The columns were designed to represent the end-regions of ductile planar reinforced concrete walls. Chai and Elayer (1999) documented the influence of the width of the cracks and of the thickness of the specimens. Besides, this study confirmed that the maximum tensile strain has a significant impact on the lateral stability of these members. An equation was developed for estimating the maximum tensile strain based on a kinematic relation between the axial force and the response of the axial strain, and the axial strain versus the out-of-plane displacement. Moreover, experimental results showed that the equation is conservative in terms of predicting the maximum tensile strain, and the equation can be incorporated into an existing design procedure for determining the minimum wall thickness.

Abdullah & Wallace (2019) found out through studying 164 walls that the main parameters that impact drift capacity are the ratio of neutral axis depth to width of the compression zone c/b, the ratio of wall length to width of compression zone l_w/b (wall slenderness), and the ratio of the maximum shear stress ratio. The correlation coefficients of the mentioned parameters to wall drift capacity are respectively 0.66, 0.56, and 0.30. It was also discovered that the configuration of boundary transverse reinforcement (use of overlapping hoops or a single parameter hoop with intermediate crossties) also significantly impacts wall drift capacity for low shear stress values ($v_{max}/\sqrt{f_c'}$ psi < 5), as for higher values few tests exist to evaluate the impact.

In another experimental study by Parra and Moehle (2017), it was shown that depending on several variables, the shear walls had a tendency to buckle under tension and compression load cycles. These primary variables are the maximum tensile strain experienced by the member prior to axial compression, the slenderness ratio kh_u/b of the wall boundary, and whether the structural wall specimens had one or two curtains of reinforcement.

Moreover, Segura & Wallace (2018) showed that larger c/b values reduce drift capacity since thicker walls ensure a wider spread of plasticity and provide increased lateral stability.

In addition to that, it was observed that the increase in shear stress demand had a significant impact on drift capacity. This was proved by Kolozvari et al. (2015) who demonstrated that shear transfer from compressive struts to flexural compression zone results in higher concrete compressive strains than those due to bending and axial load alone.

Therefore, there is a need for rehabilitating these deficient shear walls in order to enhance their reversed cyclic response.

According to Priestly et al. (1994), structural collapses during earthquakes in the 1970s were mainly the result of inadequate shear strength and poor confinement in columns. The methods used back then to improve column performances were mainly consisting of increasing the column cross-sections. This has led to the increase in column dimensions which caused several issues with the practicality and functionality of the building. An alternative to the mentioned technique is the use of carbon fiber laminates to enhance the confinement and thus the overall performance of the column without disrupting functionality and dimensions.

The first reported application in the literature of CFRP retrofit of structures occurred in Switzerland, Lucerne to repair the Ibach Bridge in 1991 by Meier (1995). The bridge had some prestressing cables damaged in the process of installing traffic lights. It was repaired with three CFRP sheets which are 15 cm wide, 500 cm long, and 1.75 mm thick. The total weight of the strips was around 6.2 kg compared to the 175 kg of steel needed for the same repair. Furthermore, the installation was carried out using a mobile platform, eliminating the need for scaffolding in other methods. Besides, the bridge was tested using an 840 KN moving load proving the repair method's success.

In this study, Ghosh and Sheikh (2007) conducted an experimental study to determine the effectiveness of a carbon fiber-reinforced polymer (CFRP) jackets retrofit process in strengthening and repairing poorly confined and detailed columns. They built and tested 12 reinforced concrete columns, 6 with circular cross-sections and 6 with square cross-sections, to simulate existing reinforced concrete columns encountered in the field that

lacked lateral strength and ductility. These columns were subjected to a combined constant axial loading and reversed cyclic lateral loading simulating a seismic event. This retrofitting method was found to be cost-effective, long-lasting, and easy to implement. Furthermore, this technique demonstrated its effectiveness in enhancing the seismic performance of deficient columns. When strengthening these columns through the use of CFRP jackets, their ductility, flexural strength, and energy dissipation capacity were significantly improved.

Moreover, Kim et al. (2011) investigated the use of Carbon Fiber Reinforced Polymer material to repair and strengthen lap splice deficiencies in large-scale reinforced concrete columns. In this study, square and rectangular RC columns were fabricated and were tested as-built and after rehabilitation. Two types of lateral loading were applied to the column specimens: monotonic and cyclic loading. The experimental results showed that columns exhibited good performance after rehabilitation. It was observed that after the rehabilitation of the columns using a combination of CFRP jackets and CFRP anchors, the lap splice behavior was successfully improved, the tensile capacity of the longitudinal bars was developed, and the deformation capacity and strength of the rehabilitated columns were significantly improved. Besides, test results showed that the application of this approach could not be limited to the columns only because CFRP materials can improve the performance of other RC elements, such as walls and beams, which may have inadequate lap splices.

Meier (1987) and Kaiser (1989) performed four beam tests on 2 m beams and Ladner (1990) performed four beam tests on 7 m beams. The beams had deficient steel reinforcement and thus low strength. They were strengthened with 1 mm thick CFRP

laminates and epoxy. It was found that the 2 m strengthened beams sustained double the ultimate load of the control beam. However, in the 7 m beams, the load capacity only increased by about 22%. As for the deflection, it decreased significantly for both beam lengths. Also, it must be noted that for reinforced beams, the failure was sudden and explosive in the tensile zone. To ensure a more ductile failure mode, Meier et al. (1992) proposed that in the retrofit process, steel reinforcement should yield first, followed by CFRP strips failure, and lastly concrete compressive failure.

Khalil and Ghobarah (2005) studied two rehabilitation schemes using CFRP sheets and carbon or steel anchors for shear walls under lateral loads. Both schemes were tested and proved to be effective in increasing the ductility, shear strength, and energy dissipation capacity of structural walls.

Paterson and Mitchell (2003) constructed four shear wall specimens and tested their performance under reversed cyclic loading. They tested two of the specimens in the as-built condition and retrofitted two companion walls prior to testing. Besides, they investigated the effectiveness of the combined use of adding a reinforced concrete collar, headed reinforcement, and CFRP wrapping in the seismic retrofit of existing shear walls that had design and detailing deficiencies. The results showed that the retrofit schemes were successful in improving energy dissipation and ductility of poorly detailed shear walls.

Layssi et al. (2012) tested existing shear walls under reversed cyclic loading and examined their behavior before and after the retrofit. The shear wall specimens were poorly designed and detailed in order to simulate old reinforced concrete construction. In this research, they investigated the use and effectiveness of retrofitting using CFRP wrap to enhance the

performance of the tested shear walls. Test results showed that this retrofit technique satisfied the performance objectives. It was found that the CFRP wrap was effective in increasing the shear strength of the wall, improving the displacement ductility, improving the cumulative dissipated energy, and preventing premature failure of the lap splices in the potential plastic hinging zone; thus, achieving some yielding of the flexural reinforcement.

Shear wall behavior and retrofit studies are numerous in the literature. Several researchers tackled the responses and failure of walls with modern detailing, as well as strength deficient walls aged 50 years old or more. The retrofit techniques that were found focused mainly on increasing shear capacity and resisting shear cracking and failure. However, little research had been carried out on assessing the effectiveness of carbon fiber-reinforced polymer as a retrofit scheme to enhance the out-of-plane buckling failure mode of non-ductile shear walls. This research aims to develop guidelines for predicting the behavior of slender shear walls that are characterized by an out-of-plane buckling failure mode, similar to the failures observed after the Chile earthquake, and to determine how using CFRP laminates to enhance the confinement at wall boundaries will affect the failure response, drift capacity, and overall strength of the shear wall. This will be implemented by subjecting two full-scale wall specimens to in-plane lateral cyclic loading. The first will be the control specimen where severely damaged sections at the base of the wall will be determined, then these sections will be marked on the second specimen and reinforced with CFRP laminates.

CHAPTER THREE

METHODOLOGY

3.1 Research Aim and Objectives

The aim of this research is to investigate a rapid and effective method for correcting critical structural deficiencies in thin reinforced concrete shear-walls that lead to overall wall instability and extensive damage during seismic events. The objectives set forth to achieve this goal are therefore established as follows:

1. Design a strength-deficient shear wall.

2. Test the strength-deficient shear wall in the LAU structural testing facility.

3. Analyze the obtained results of the experimental tests to identify the failure mode.

4. Devise a strengthening retrofit scheme using CFRP laminates and anchors and apply it to a second shear wall specimen identical to the first.

5. Test the retrofitted wall and compare the results to those of the first wall to demonstrate the effectiveness of the retrofit scheme.

6. Optimize the retrofit design by comparing strains in the CFRP sheets to maximum allowable strains and propose retrofit design guidelines.

3.2 Research significance

The location of Lebanon on the east coast of the Mediterranean Sea imposes the need for proper consideration of seismicity in building design. Salameh et al. (2016) summarized the last earthquake, magnitude, and return period of each of the three faults that Lebanon

lies upon. By adding the numbers, one can see that the Mt Lebanon fault has had enough time to accumulate enough energy to produce an earthquake of magnitude 7 on the Richter scale in the near future. An earthquake of this magnitude can be catastrophic in Lebanon's case due to the poorly designed and densely populated old buildings. Another problem is that although a law that forces the implementation of the proper seismic design was passed in 2004, the enforcement of this law is almost non-existing. In addition to the old structures, the newly built ones also are strength-deficient in resisting lateral loads and require proper strengthening. The significance of this research lies in proposing effective and feasible guidelines for the retrofit of existing strength-deficient shear walls—especially in the Beirut area in order to provide lateral stability of boundary regions during seismic events. Thus preventing or minimizing severe damage or even collapse of structures and giving more crucial time for evacuation and saving people's lives.

3.3 Experimental Setup

3.3.1 Equipment and software needed

The experiment was conducted using a Reaction Wall and Strong Floor (RWSF) testing setup in the Engineering Laboratories and Research Center (ELRC) at the Lebanese American University (LAU). This equipment can perform quasi-static and pseudo-dynamic two-dimensional earthquake simulations on full-scale structural concrete members and building components such as girders, piers, and shear walls. It can also handle a variety of axial and lateral loading scenarios. The RWSF system consists of the hydraulic power unit, where the hydraulic energy is produced to the system, with its electric panel and the actuator assembly, and an electric actuator control panel as illustrated in Fig. 1. The hydraulic unit and actuator assembly are controlled by the electric

panels that contain switches and a built-in PC. The actuator assembly is made up of a base plate fixed to the wall by four M24 tie rods. Two hydraulic actuators procured by Bosch have a maximum capacity of 1200 KN and a maximum frequency of 10 Hz. A piston-cylinder is capable of producing 900 kN push force and 565 kN pull force. The actuator is connected to the base plate by a clevis bracket that ensures the alignment of the force during the test. In addition, a load cell that can read loads in compression and tension up to 120 kN. Moreover, experiments are applied and monitored from the control panel where the progress and results are displayed on the software installed on the built-in PC.
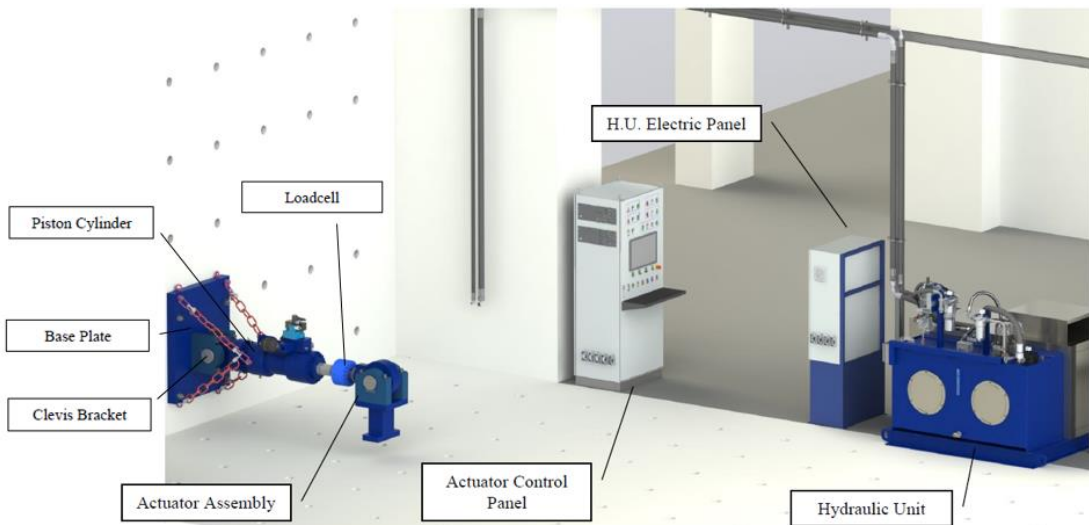
Fig. 1 Description of the RWSF Machine

To measure the strain vs applied load, sixty two pre-wired strain gauges are used for the measurement of the strain with respect to the applied load. The pre-wired strain gauges are manufactured by Omega. The chosen model is KFH-10-120-C1-11L1M2R that have a linear 10 mm grid with two 1-meter leads and 120 Ω resistance. The strain gauges were connected to the data acquisition using extension cables. Figure 2 shows a sample of the used pre-wired strain gauge.
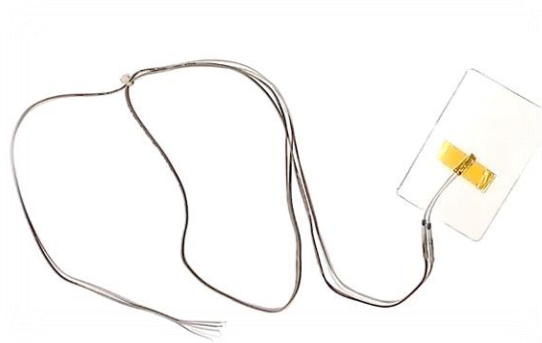
Fig. 2 Pre-wired strain gauges

In order to monitor the displacement of the shear wall specimens in 3D, two cameras were placed parallel to each other on the same tripod and had a center-to-center distance of 27 cm, as shown in Figure 3. Both cameras were placed facing toward the wall. The cameras are manufactured by Imperx. The chosen model is IMPERX CXP-C5190C where the cameras have a 4-channel C5190 CXP-6 CoaXPress output interface and a resolution of 25 MP. The cameras were connected to the PC using a Kaya Komodo 8-channel frame grabber. This frame grabber was manufactured by kaya Instruments and it was fully compatible with our cameras. Using the Vision Point software, both cameras can be triggered at the same time. Some parameters were modified in the settings of the cameras and frame grabber. For example, the maximum exposure time was changed to 10,000micro-seconds, the f-stop was changed to 5.6, and the frame rate was set to be 1 frame per second. The acquired images are monochrome because this type has better resolution and these images are stored in (.raw) format for later processing. This setup allows the research team to measure all the movement happening in the plane of the sensor. In fact, we are able to measure the wall displacement and trace the progression of cracking. In addition, the out-of-plane displacement can be obtained by doing 3D measurements where both cameras are used to triangulate the out-of-plane movement.

Fig. 3 Two Imperx cameras

3.3.2 Calibration

A stiff planar rectangular board was used for calibrating our cameras. The calibration board had a white matte background and black circular dots printed in a square grid array where their center-to-center distance was equal to 3 cm, as depicted in Figure 4. The calibration process requires that the calibration board be positioned in multiple orientations. For example, the board should be positioned straight such that it faces normal to the line of sight and should be positioned inclined at different inclinations such as being inclined to the left, right, down, and up. For each orientation, 9 images were acquired where the calibration board position was moved over the entire camera's field of view to have full coverage of the field of view. Once the process of capturing images was complete, a calibration procedure is performed using special software.
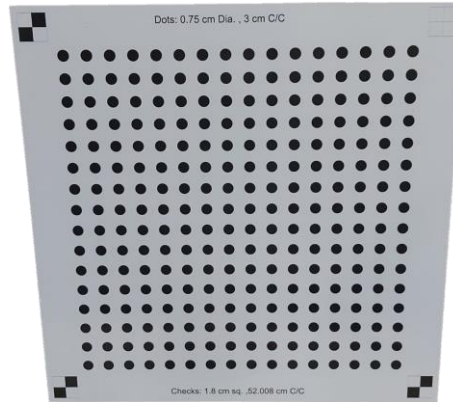
Fig. 4 Calibration Board

3.3.3 Wall Design

The test specimens consist of two walls that represent typical shear walls of old buildings in the Beirut area, which are not designed up to building codes—specifically minimum wall thickness, minimum steel layers, minimum bar diameters, and detailing of boundary elements. The two walls have identical dimensions: The height from the top of the foundation to the top of the wall is 2900 mm, the wall thickness is 125 mm, and are wall length is 1600 mm. The walls are T-shaped, having a 200 mm thick and 500 mm long flange at the west end. The longitudinal reinforcement consisted of a single layer of seven 10 mm diameter bars spaced at 250 mm in the web, and eight 16 mm diameter bars in the flange. The transverse reinforcement consists of twenty-two 10 mm diameter bars spaced at 125 mm. The deformed steel bars used for the reinforcement of the shear wall specimens had a yield strength of 608 MPa and the concrete had a compressive strength of 20 MPa. The dimensions and detailing of the walls are shown in Fig. 5. Since the wall has only one layer of steel, the vertical bars were placed on the centerline of the section, while the horizontal ones had a 10 mm eccentricity to the right from the flange side as shown in Fig. 5 (b).
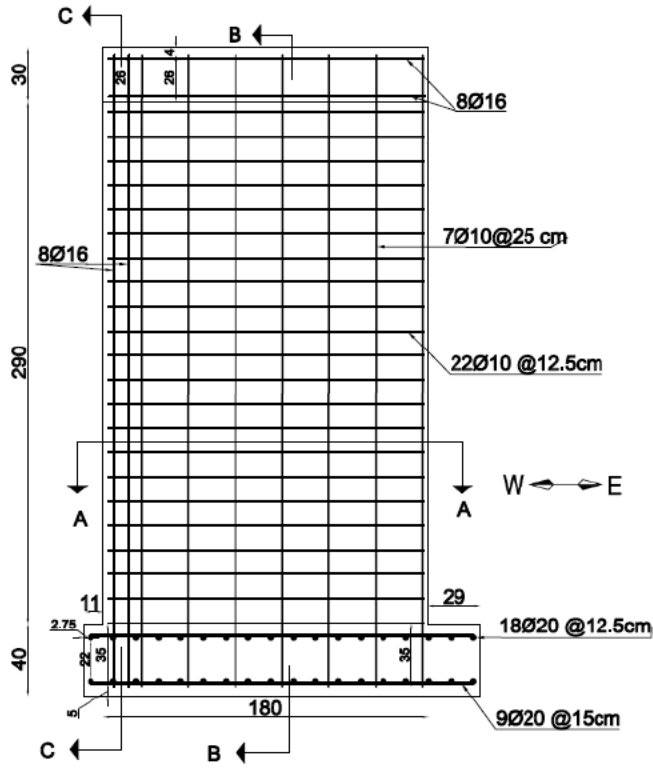
PLAN VIEW

(a)
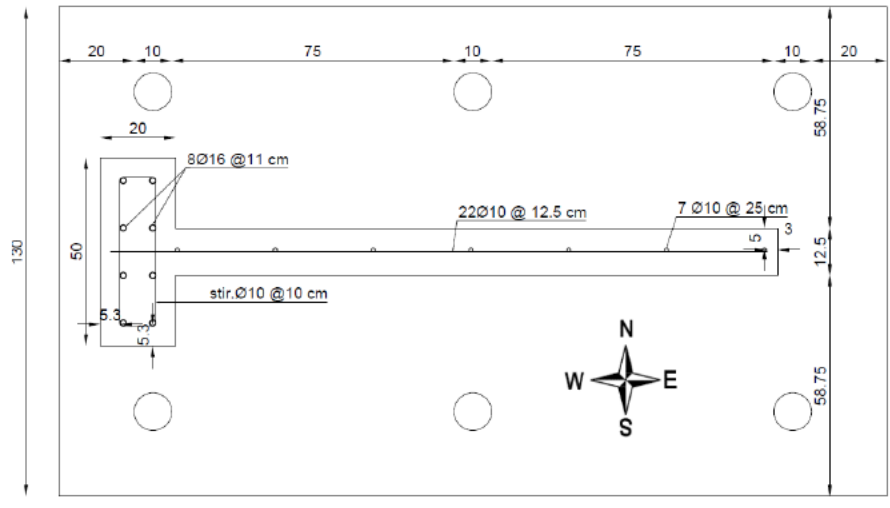
Section A-A

(b)

Fig. 5 Wall Specimen Dimensions and Reinforcement Details (all dimensions in mm)

In addition, the foundation which is 2200 mm long, 1300mm wide, and 400mm thick was connected to the strong floor through six prestressed rods. The foundation was designed for maximum rigidity to provide proper anchorage in the wall in order to avoid the reduction of energy dissipation, as indicated by Greifenhagen et al. (2005) and was heavily reinforced to represent a fixed boundary to the slender shear wall specimens and to minimize its damage when the walls are subjected to cyclic loading.

The wall dimensions were selected in such a way so as to achieve a flexural mode of failure, all while taking into consideration the space constraints imposed by the test location. This was done through multiple iterations until the results confirmed the desired mode of failure when using the ACI equations. First, the wall's shear strength was calculated using Equation (1) [ACI Equation 18.10.4.1]:

$$V_{yE,d} = A_{cv}\left(\alpha_c \lambda \sqrt{f'_{cE}} + \rho_t f_{ytE}\right) \leq 10 A_{cv}\sqrt{f'_{cE}} \qquad (1)$$

Where A_{cv} is the area of concrete section bounded by web thickness and wall length, α_c is the shear span ratio, f'_{cE} is the concrete compressive strength, and ρ_t and f_{ytE} are the transverse reinforcement ratio and yield strength, respectively.

Second, the shear friction at wall base was calculated using Equation (2) [ACI Equation 22.9.4.2]:

$$V_{yE,f} = \mu\left(A_{vf} f_{ylE} + P\right) \leq 0.2 f'_{cE} A_c \qquad (2)$$

Where A_{vf} is the area of reinforcement crossing the wall/foundation interface, f_{ylE} is their corresponding yield strength, A_c is the area of concrete section resisting shear transfer, μ

is the coefficient of friction taken as 0.6 as in ACI 318-14 Table 22.9.4.2, and P is the axial load.

Third, the wall shear demand is given by Equation (3):

$$V_{@MyE} = \frac{M_{yE}}{SSR \times l_w} \tag{3}$$

Where l_w is the total length of the wall. After calculating the shear strength, friction, and demand, the dominating failure behavior of the wall can be predicted using Table 1. Accordingly, dominating flexural behavior was determined for the walls considered in this study with a factor of safety of 1.25.

Table 1 Criteria for determining the expected wall dominant behavior. Abdullah and Wallace (2021)

Criterion		Expected Dominant Behavior
$V_{yE}/(\omega_v V_{@MyE}) < 1.15$	$V_{yE,d} \le V_{yE,f}$	Diagonal shear -controlled
	$V_{yE,d} > V_{yE,f}$	Sliding shear-controlled
$V_{yE}/(\omega_v V_{@MyE}) \ge 1.15$		Flexure-controlled

Note: V_{yE} is the least of $V_{yE,d}$ and $V_{yE,f}$ per Eq. 2 and Eq. 3, respectively, and ω_v is computed from Eq. 4.

3.3.4 Testing Program

The experimental testing program on reinforced concrete shear walls was carried out at the LAU ELRC structures lab. A horizontal actuator was used to subject the wall to cyclic in-plane loading. At the top of the wall a rigid 50 x 30 cm beam provides the needed integrity to the brittle wall top while testing and to ensure that the whole wall section is resisting the cyclic loads. The actuator is connected to the top beam at 3050 mm from the top of the foundation using 4 prestressed rods and two steel plates sandwiching the beam from both sides. Fig. 6 illustrates the general test setup used in the experiment.
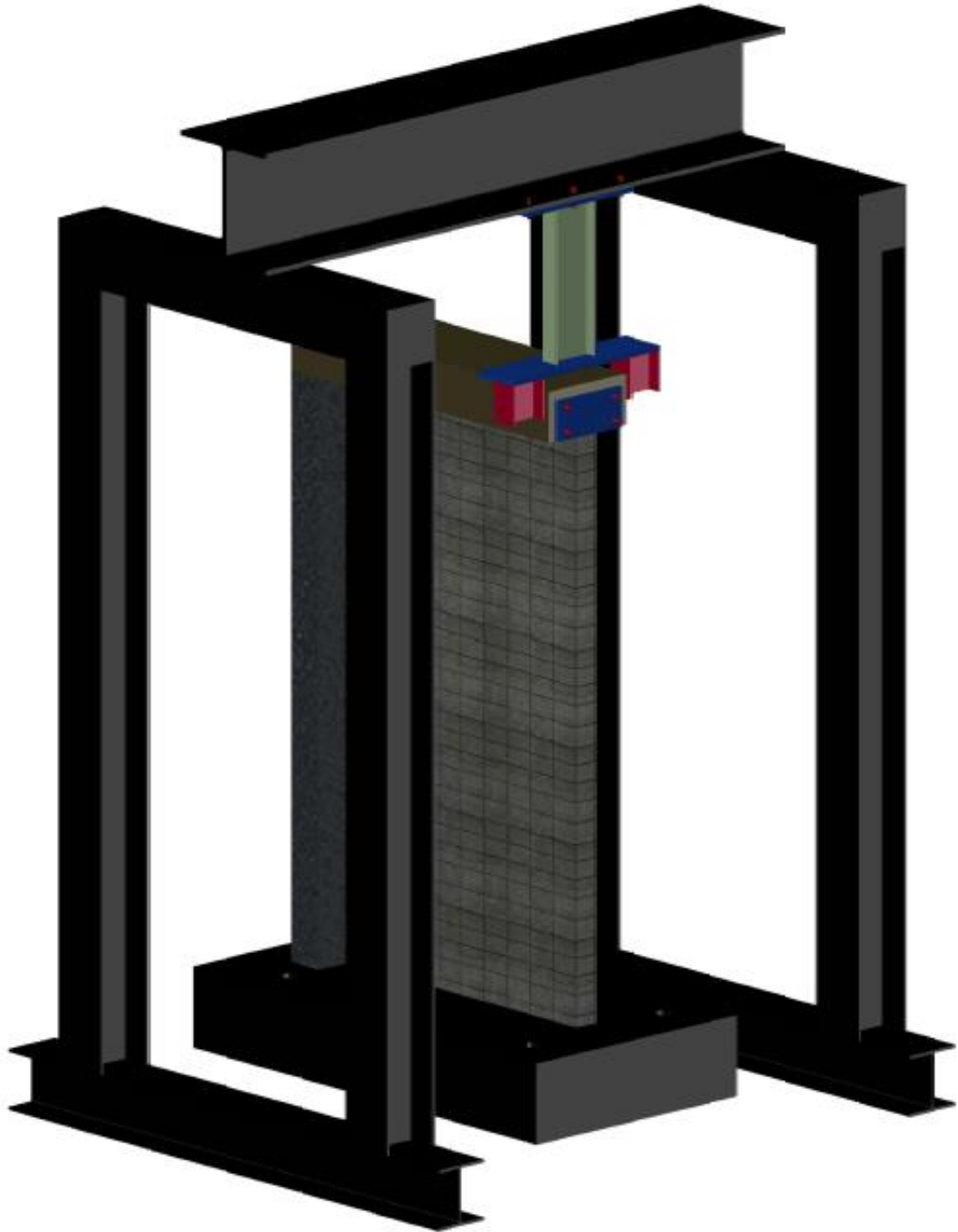
Fig. 6 3D representation of the test setup

The loading protocol consisted of a reversed cyclic loading, imposed by the horizontal actuator in displacement control. Two fully-reversed cycles were applied at each target drift, according to the following incremental drifts: $\pm\, 0.05\,\% \rightarrow \pm\, 0.1\,\% \rightarrow \pm\, 0.15\,\% \rightarrow \pm\, 0.25\,\% \rightarrow \pm\, 0.35\,\% \rightarrow \pm\, 0.5\,\% \rightarrow \pm\, 0.75\,\% \rightarrow \pm\, 1\,\% \rightarrow \pm\, 1.5\,\% \rightarrow \pm\, 2\,\% \rightarrow \pm\, 2.5$ for the as-built wall (W). A full description of the drift protocols including load stages (LS) is represented in Fig. 7 and Fig. 8.

During the loading phases, the applied forces were recorded by load cells in the actuators, and data were collected from the strain gauges on the reinforcing bars. Out of the 31 strain gauges, 14 strain gauges, which are the 1/B, 1/C, 1/D, 1/E, 2/A, 2/B, 2/C, 2/E, 3/C, 3/D, 3/E, 4/D, 6/C, 7/B, were properly functioning in the as-built wall. The reason behind that is that the strain gauges wires were cut during the concrete pouring process, especially the gauges at the wall base. Figure 9 illustrates the location of the strain gauges on the reinforcing bars and the highlighted ones indicate the working strain gauges. The two cameras, which were connected to a data acquisition software, recorded 3-dimensional displacements of high contrast targets placed along the face of the wall to monitor in-plane and out-of-plane displacements and to trace the progression of cracking. Moreover, at the end of each drift cycle, photos of the wall were taken from eight different angles to match new observations to their respective drift value.
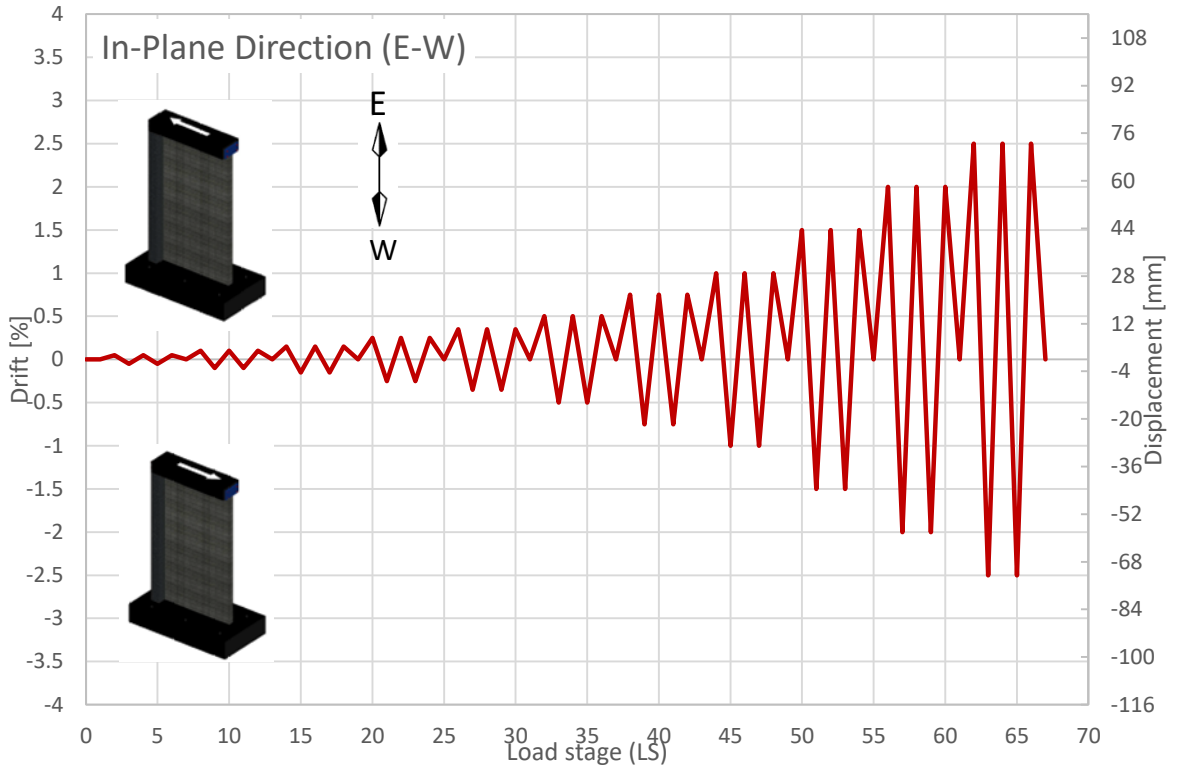
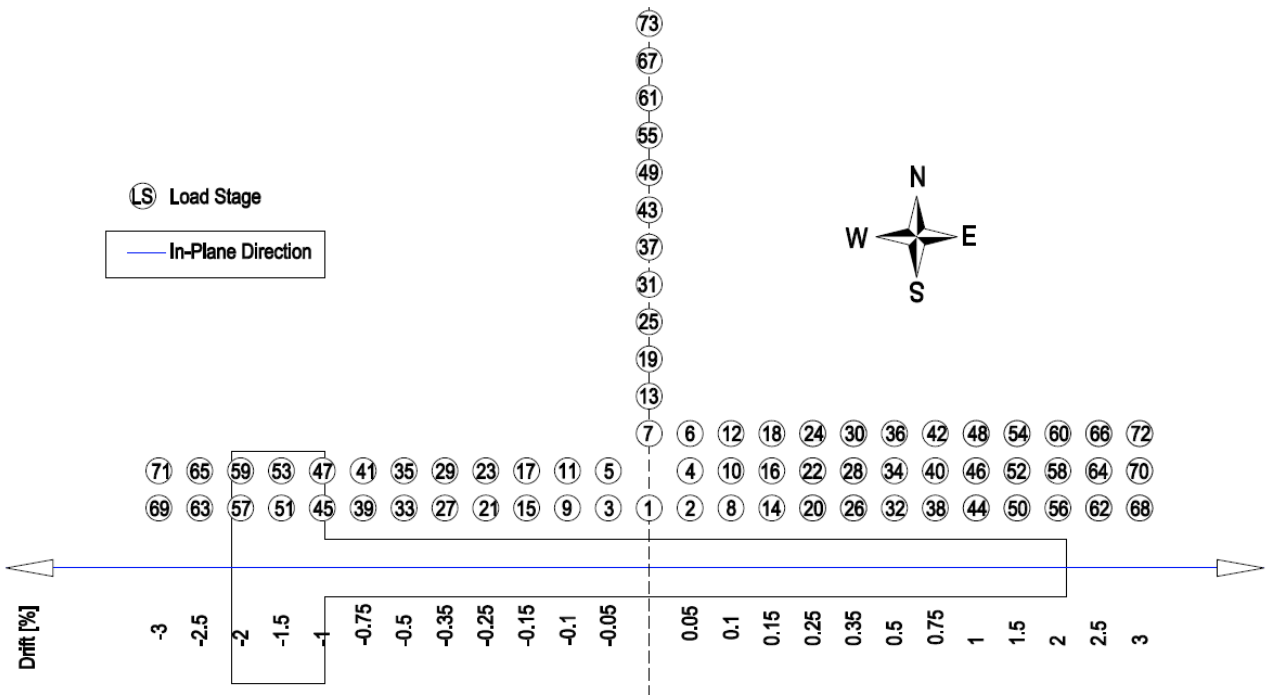*Fig. 7 Drift Protocols of the reversed cyclic load tests including load stages*

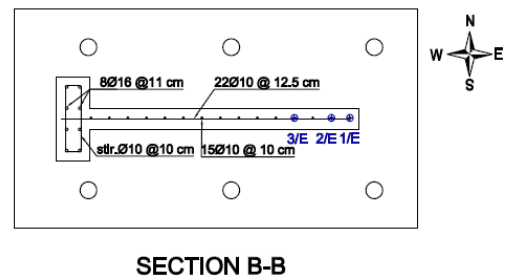

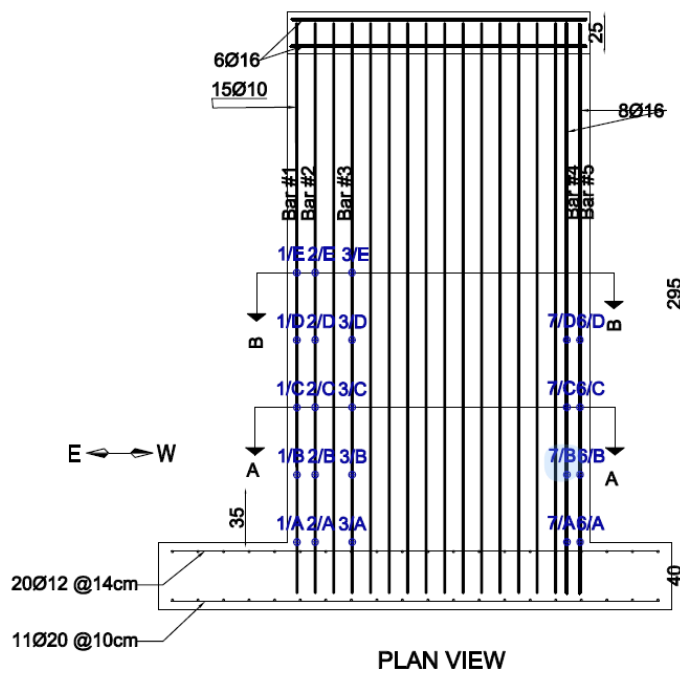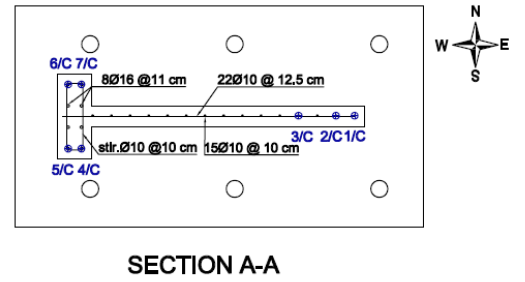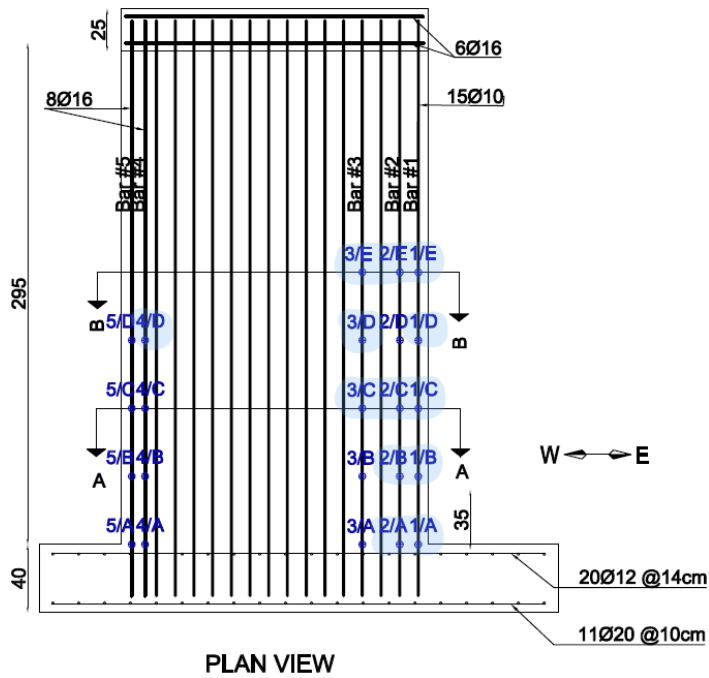*Fig. 8 In-plane representation of the loading protocols*

Fig. 9 Strain Gauges layout

CHAPTER FOUR

RESULTS AND ANALYSIS

4.1 As-built wall test observations

Starting with the first cycles, horizontal and diagonal cracks started forming in the as-built wall (W), and these cracks started propagating with the increase of displacement. During loading LS 50→LS 51 (in-plane drift amplitude: drift = ±1.5 %), the lateral buckling of wall (W) started where it was observed the opening of the crack at the wall base along with its closure during the loading cycle LS 51→LS 52. Moreover, at the end of the in-plane drift amplitude of ±2 %, the crack at the base of the wall was clearly visible as well as the small chunks of concrete that were fallen down. Finally, during loading LS 63→LS 64 (in-plane drift amplitude: drift = ±2.5 %), concrete crushing was observed at the free web edge of the wall. Following the progression of concrete crushing, the longitudinal rebars buckled towards the South at the web end of the wall during loading LS 65→LS 66; thus, leading to buckling failure, see Fig. 10(a) and Fig. 10(b). As shown in Fig. 10(c), the wall failure involved concrete crushing and buckling of the vertical rebars at the web edge.

(a)   (b)   (c)

Fig. 10 As-built wall (W) at the end of the test, after failure
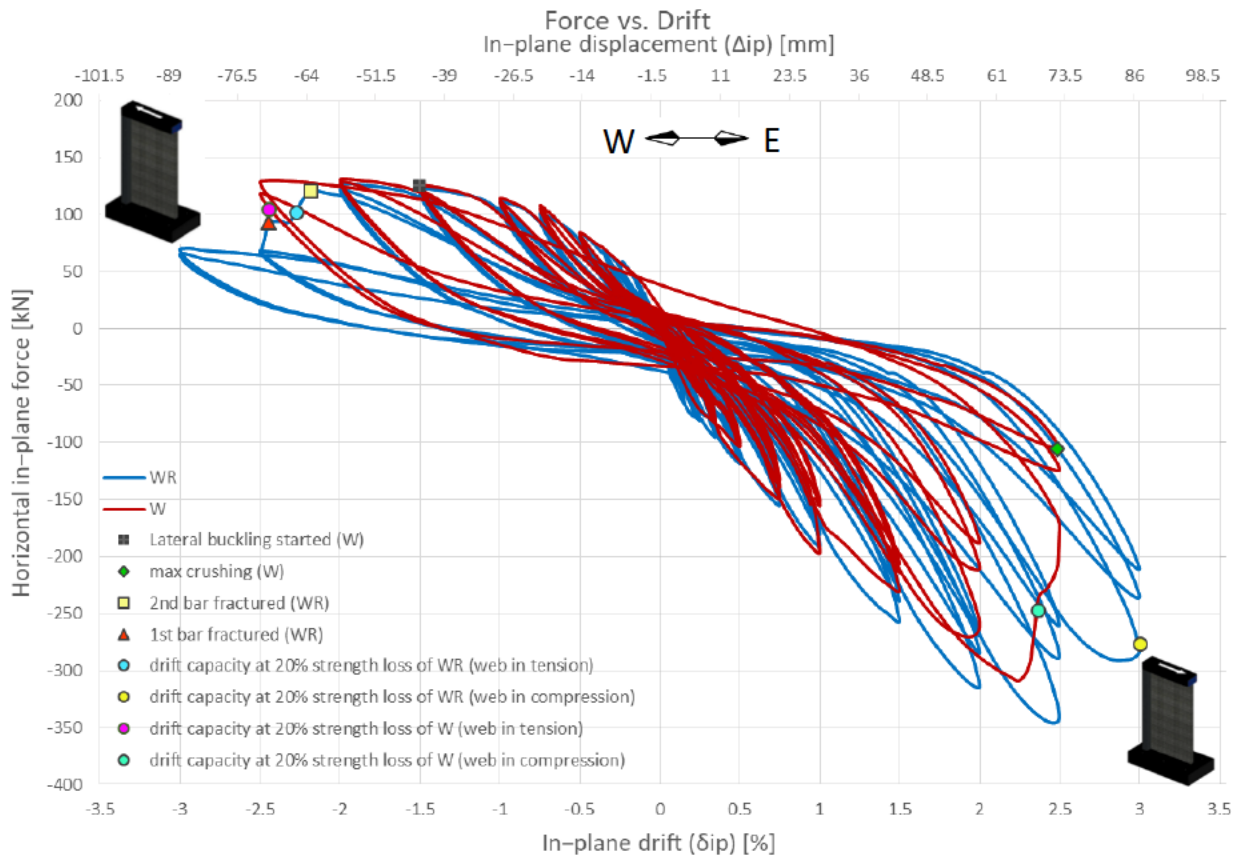
4.2 Force-displacement response

Fig. 11 In-plane force-displacement response of the as-built wall (W) and the retrofitted wall (WR)

Fig. 11 describes the in-plane force-displacement responses of the as-built wall (W) and

the retrofitted wall (WR), where it was shown that the blue curve went farther than the red

curve. This means that the retrofitted wall maintained its strength for a longer period

before it became unstable and started losing strength. However, the retrofitted wall did

not gain much of a deformation capacity increase because the longitudinal bars started

fracturing early and the retrofitted wall started losing strength at 2.5% drift. As can be

seen in Fig. 11, during loading the web in tension for an in-plane drift amplitude of ±2.5

%, it can be observed that the wall lost the first bar when the forces started dropping at -

2.2% drift. Then, when the forces dropped at around -2.4% drift, the second bar was

fractured. However, we can not define from the graph at which drift the third bar was

fractured. Maybe two bars were fractured at the same time or maybe the third bar fractured during the compression cycles.

When looking at the right side of the in-plane force-displacement response of wall W, the force capacity peaked at -308 kN during the last loading of ±2.5 at approximately 2.25% drift between LS61 and LS 62. Then, between LS62 and LS63, wall W reached 80% of its peak strength at about 2.36%. Therefore, the drift capacity at 20% strength loss of wall W is 2.36% when the web is in compression. Then, when loading from the flange to the web (between LS63 and LS64), it was observed that the as-built wall lost its strength because of the buckling of the web region. Hence, the wall started losing strength when it started losing its compression block. Finally, maximum concrete crushing was observed between LS65 and LS66 at 2.5% drift.

When looking at the right side of the in-plane force-displacement response of wall WR, the force capacity peaked at -346 kN at about 2.5% drift. Then, during the last loading cycle of ±3, it can be observed the drop of 20% of the force capacity at a 3% drift between LS68 and LS69. Therefore, the drift capacity at 20% strength loss of wall WR is 3% when the web is in compression. Besides, when loading from the flange to the web, it was observed that the retrofitted wall was losing strength between LS67 and LS68. Because the web region was in compression and was still stable (did not buckle), it was concluded that the strength loss occurred when the column was in tension. In fact, an unknown factor happened on the tension side and led the wall to lose more than half its strength.

It can be concluded that the retrofitted wall had gained some deformation capacity on the right side. In fact, wall W lost 20% of its strength at 2.36% drift while wall WR got to the

same level of strength loss at 3%. Therefore, the drift capacity increased by 27% when the wall was retrofitted.

Furthermore, when looking at the left side of the in-plane force-displacement response of wall W, the force capacity peaked at 131 kN at -2% drift. Then, during the last loading cycle of ±2.5, wall W reached 80% of its peak strength at about -2.45% drift between LS65 and LS 66. Therefore, the drift capacity at 20% strength loss of wall W is -2.45% when the web is in tension. In addition, it was noticed the section yield at -0.6% drift because before this drift value, the force is increasing as the displacement increases. However, after that drift, the forces stops increasing as the displacement increases. Then, it flattened at 131 kN.

However, when looking at the left side of the in-plane force-displacement response of wall WR, the force capacity peaked at 127 kN at -2% drift. Then, during the loading cycle of ±2.5% drift, wall WR reached 80% of its peak strength at about -2.27% drift between LS62 and LS63. Therefore, the drift capacity at 20% strength loss of wall WR is -2.27% when the web is in tension. This strength loss was due to the fracture of the first bar at -2.2% drift. Then, a second bar was fractured at -2.4% drift. Then, the force capacity maintained stable levels throughout the last loading cycle of ±3.

It can be concluded that the retrofitted wall did not gain much deformation capacity on the left side when loading from the web to the flange. In fact, wall W lost 20% of its strength at -2.45% drift while wall WR got to the same level of strength loss at -2.27%. Therefore, the drift capacity had decreased by 7% because of the fracture of three longitudinal steel bars in the web of the retrofitted wall.

4.3 Strain gauges results

Figure 9 shows the placement of the strain gauges on the longitudinal steel bars. **Error! Reference source not found.** through Fig. 24 show the forces versus strain plots that were recorded by the data acquisition system for the as-built wall (W).

The plots of the strains located in the web of the as-built wall were illustrated in Figure 12 through Figure 22. Positive strains mean that the wall was experiencing positive displacements and the web was loaded in compression; whereas, negative strains mean that the wall was experiencing negative displacements and the web was loaded in tension. It can be concluded that the strains are higher when the web is loaded in tension than those when the web is loaded in compression. In addition, the strain values are increasing when moving toward the web end region and when moving down toward the wall base. It was also observed that the maximum tensile strain demands in the web had exceeded the yielding strain which is equal to 3 millistrain, which implies that these steel bars had yielded.

The plots of the strains located in the flange of the as-built wall were illustrated in Figure 23 and Figure 24. Negative strains mean that the wall was experiencing positive displacements where the web was loaded in compression; whereas, positive strains mean that the wall was experiencing negative displacements where the web was loaded in tension. It can be noticed that the strain values were higher in tension when the web was loaded in compression. In addition, the maximum tensile strains were lower than the yielding strain; therefore, the steel bars in the column did not yield.
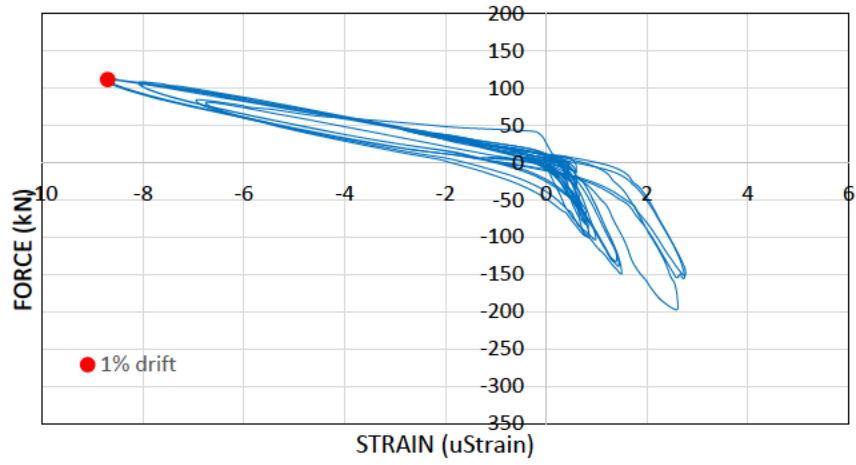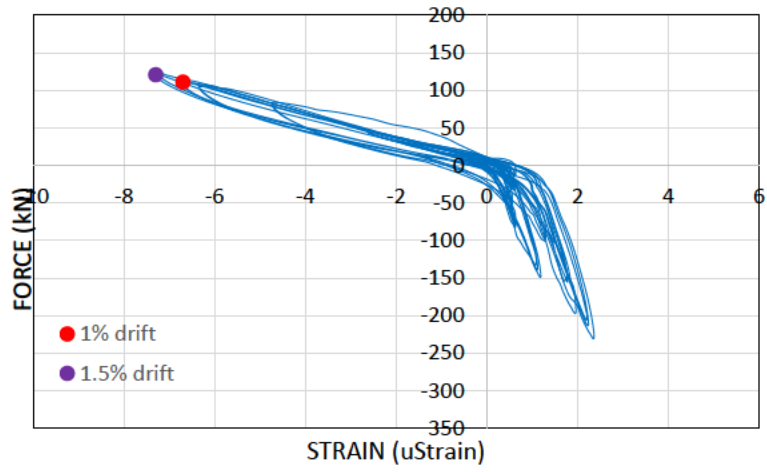
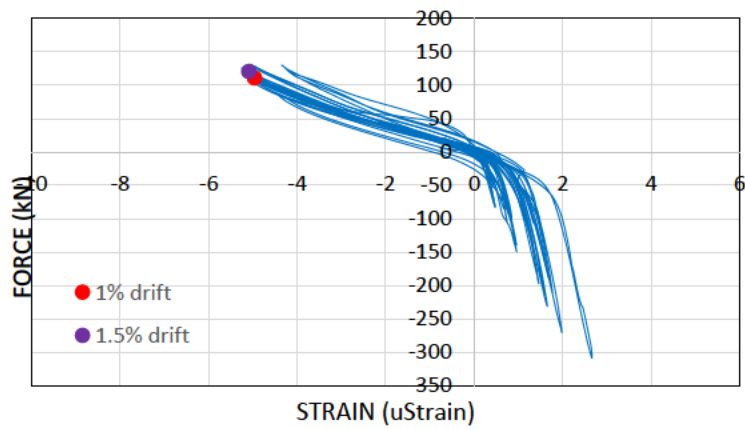*Fig. 12 Strain 1/B (W)*
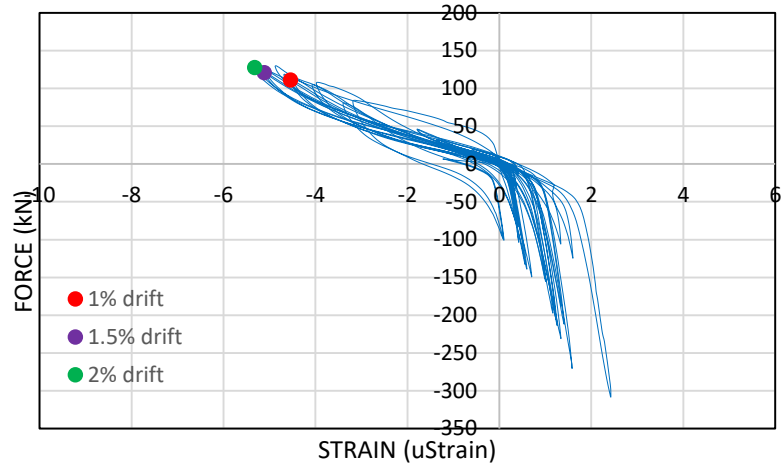

Fig. 13 Strain 1/C (W)
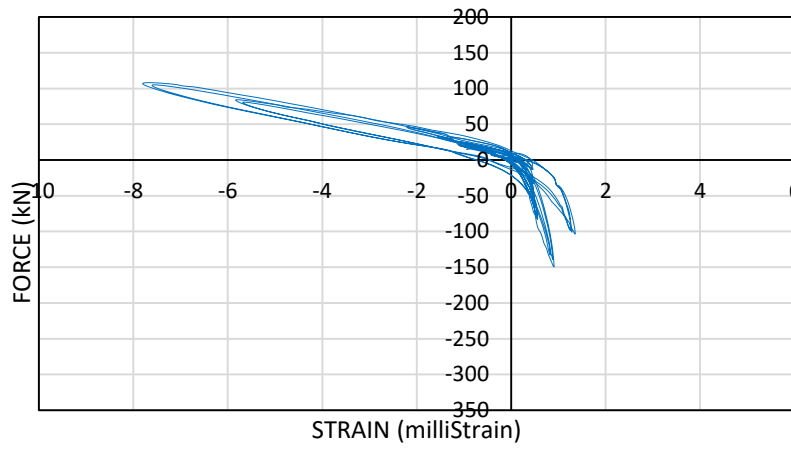

Fig. 14 Strain 1/D (W)
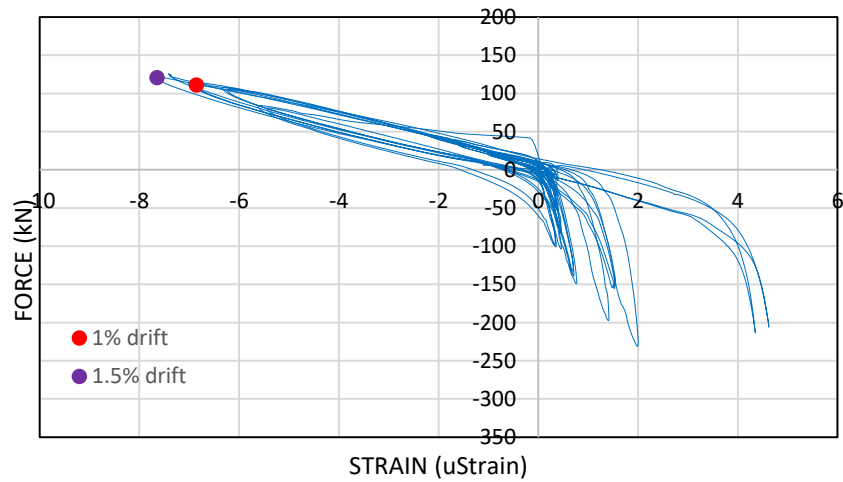
Fig. 15 Strain 1/E (W)
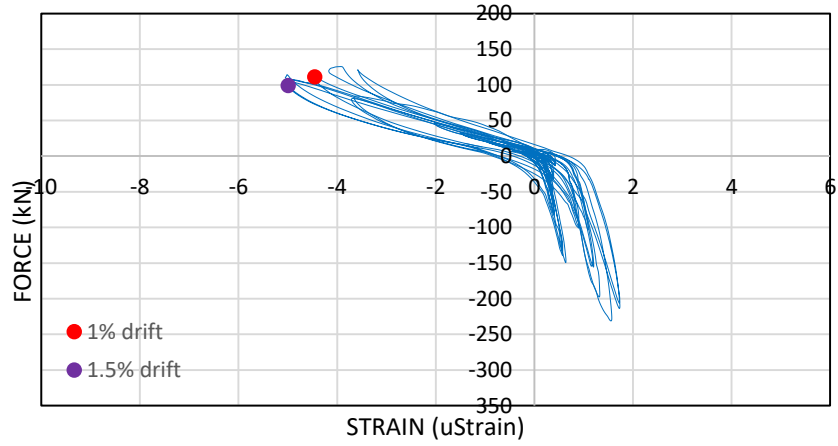

Fig. 16 Strain 2/A (W)
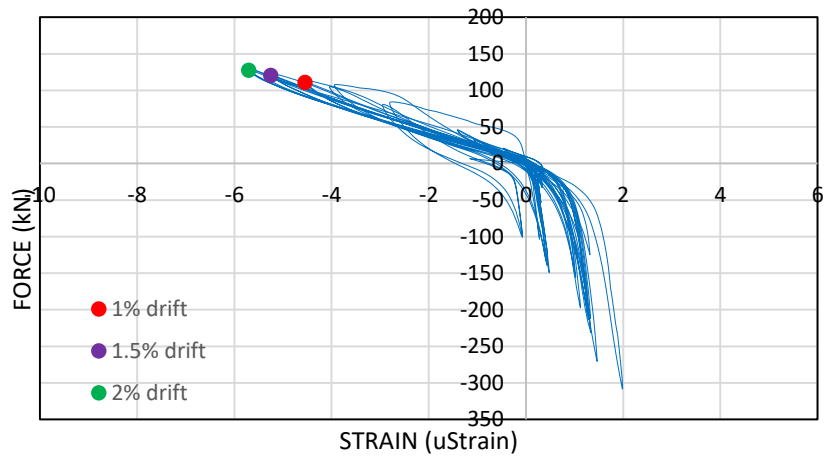

Fig. 17 Strain 2/B (W)
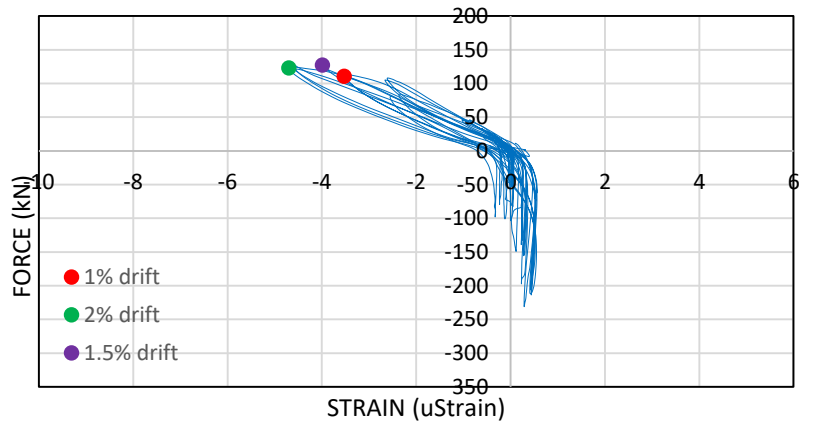
Fig. 18 Strain 2/C (W)
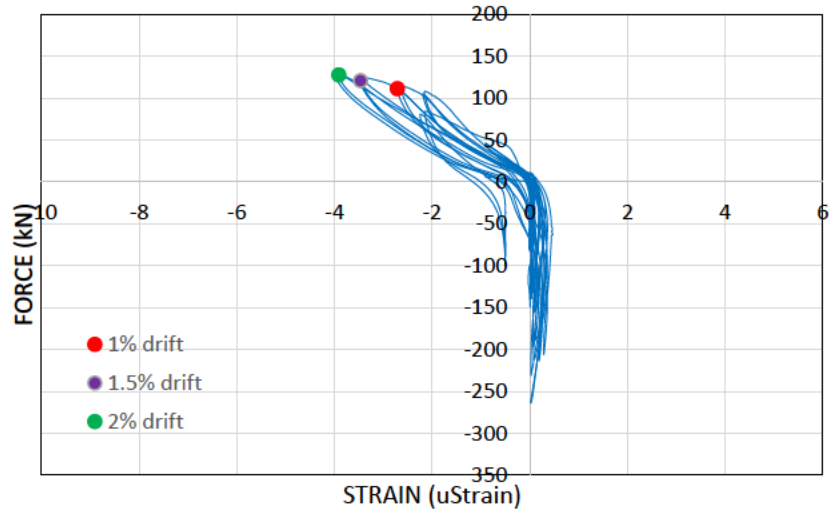

Fig. 19 Strain 2/E (W)

Fig. 20 Strain 3/C (W)
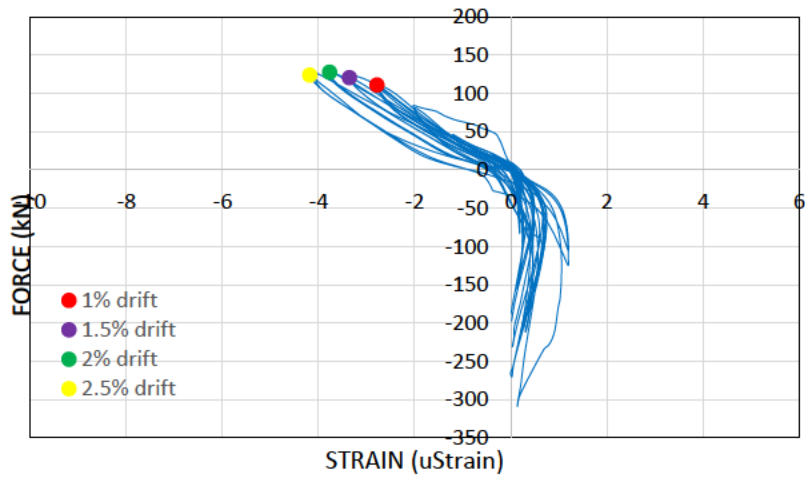
Fig. 21 Strain 3/D (W)
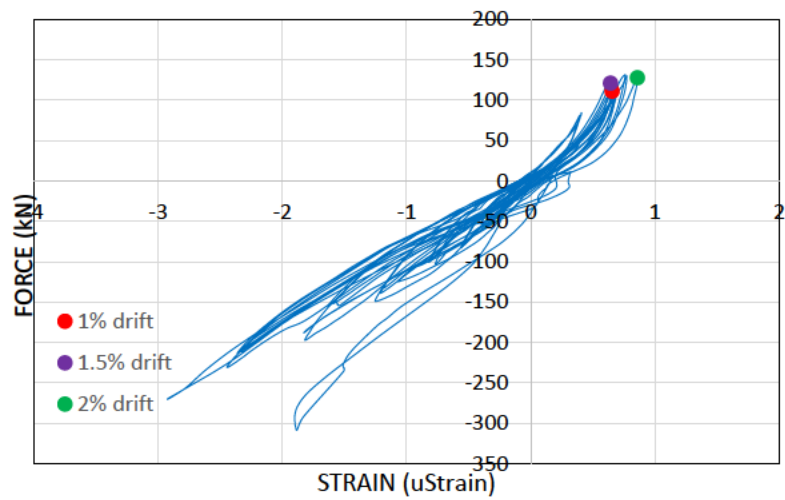

Fig. 22 Strain 3/E (W)
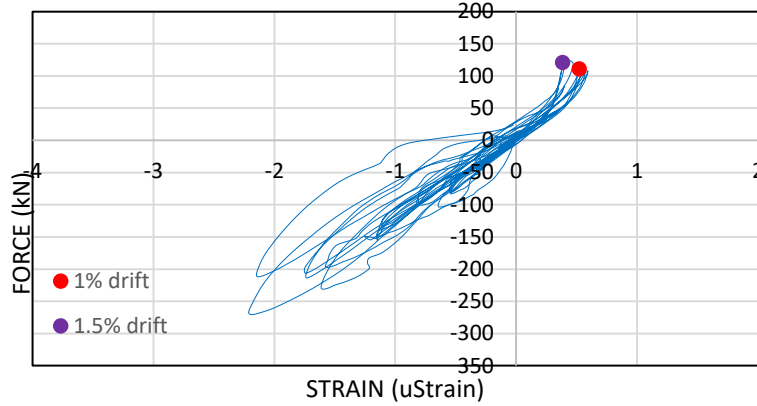

Fig. 23 Strain 4/D (W)

34

Fig. 24 Strain 7/B (W)

The strain measurements obtained from the data acquisition for the strain gauges placed on longitudinal bar #1, 2, and 3, which are located in the web (see Fig. 9), are presented in (c)

Fig. 25.

This figure illustrates the strain readings reported up to 1.5% drift amplitude because after that drift, damages in the as-built wall rendered the strain readings unreliable. Data from malfunctioning strain gauges was removed.

For the strain gauges placed on longitudinal bar #1 and 2, it was observed that the reported strain measurements reached the strain yield, calculated using Equation (4), at 0.5% drift amplitude.

$$\epsilon = \frac{Fy}{E} = \frac{608.11\ MPa}{200*10^3\ MPa} = 0.00304 = 3\ \text{milliStrain} \quad (4)$$

For the strain gauges placed on longitudinal bar #3, the calculated strain yield was reached at 1% drift amplitude at a height of 80 cm, while a similar strain was reached at 1.5% drift amplitude at a height between 120 and 160 cm.
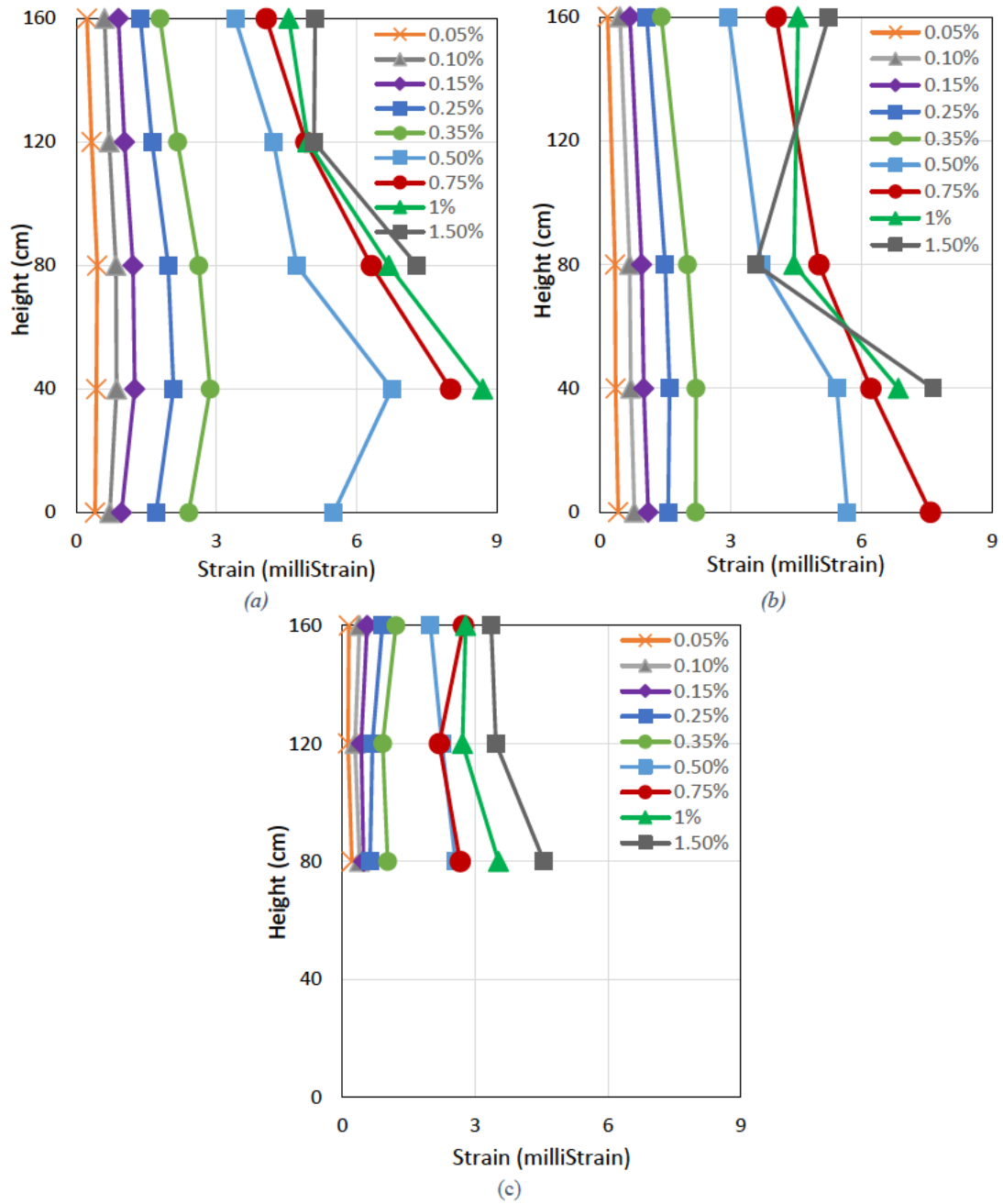
Fig. 25 Strain measurements for the strain gauges placed on longitudinal bar: (a) #1, (b) # 2, and (c) #3

4.4 Out-of-plane buckling
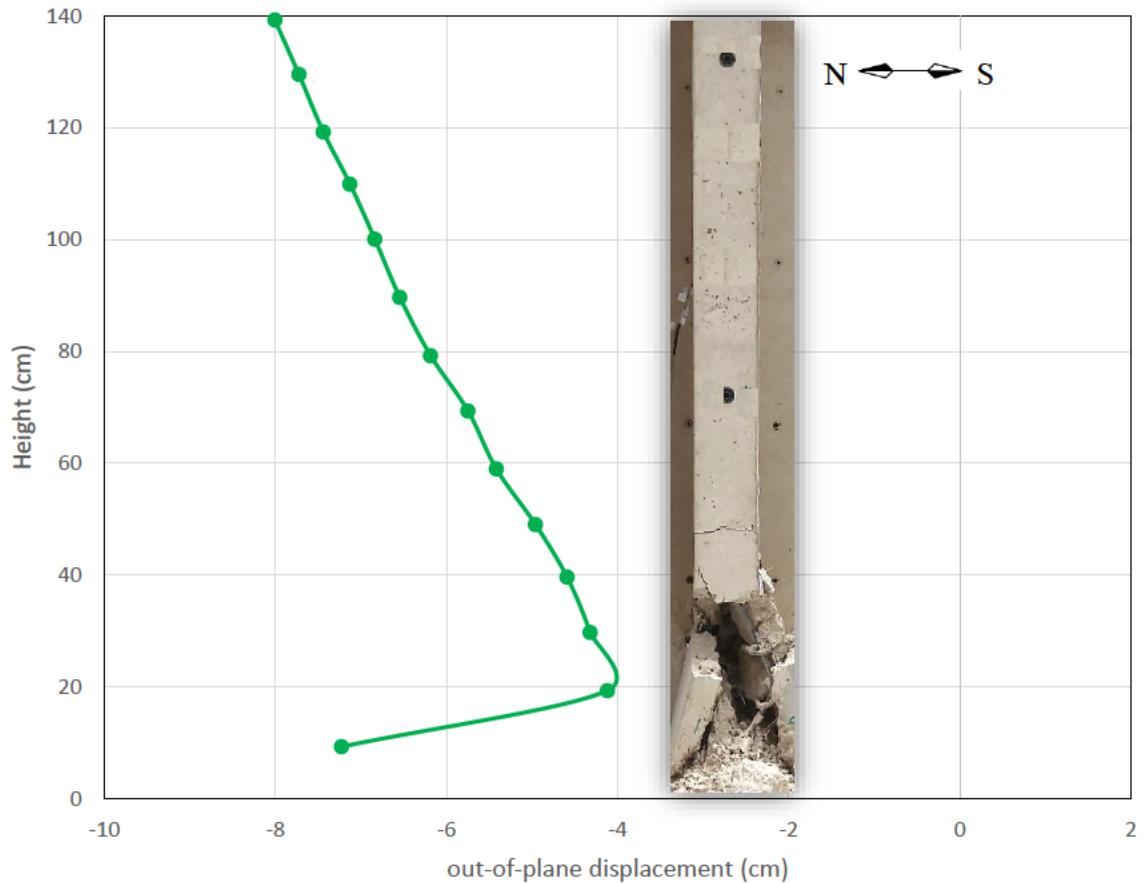
Fig. 26 Relative Out-of-plane buckling of the as-built wall (W)

Figures 26 and 27 show the relative out-of-plane buckling of the as-built wall (W) and retrofitted wall (WR), respectively. For the as-built wall, the out-of-plane buckling can be clearly shown in Figure 26 where the relative out-of-plane displacement was 3 cm toward the South over a height of 20 cm. The large out-of-plane displacement shown in the web edge occurred due to the buckling of the longitudinal steel bars at the wall base that caused the crushing of the concrete cover of the wall. Therefore, the as-built wall had a flexure buckling failure mode when loaded under cyclic lateral loads.
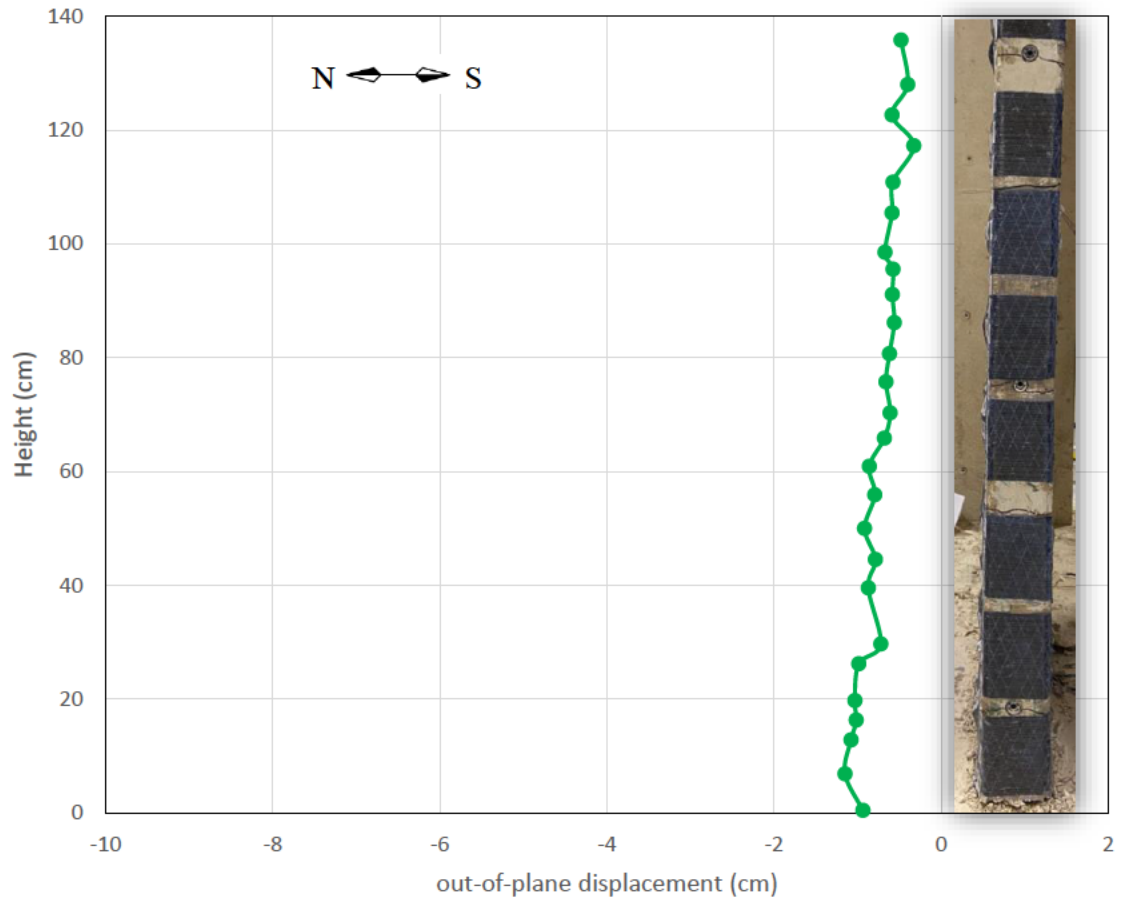
Fig. 27 Relative Out-of-plane buckling of the retrofitted wall (WR)

As shown in Figure 27, no out-of-plane buckling was present at the base of the retrofitted wall. It can therefore be concluded that when retrofitting the wall using carbon fiber-reinforced polymers sheets, the flexural behavior of the wall is enhanced. In fact, the lateral buckling was improved and the out-of-plane movements were reduced substantially. This happened because the CFRP laminates provided confinement, preserved the concrete at the web edge, and prevented the concrete from crushing under lateral cyclic loading.

4.5 Plasticity spread

Figure 28 and Figure 29 show the height versus strain of the first and second cycles of the 0.5% drift, respectively. Figure 30 and Figure 31 show the height versus strain of the first and second cycles of the 0.75% drift, respectively. The stains are calculated using the data computed from the cameras to show the wall from the camera's perspective. As illustrated in Figure 32, the strains are calculated between the targets located at the end of the wall; thus, a reading was computed between the targets every 10 cm.
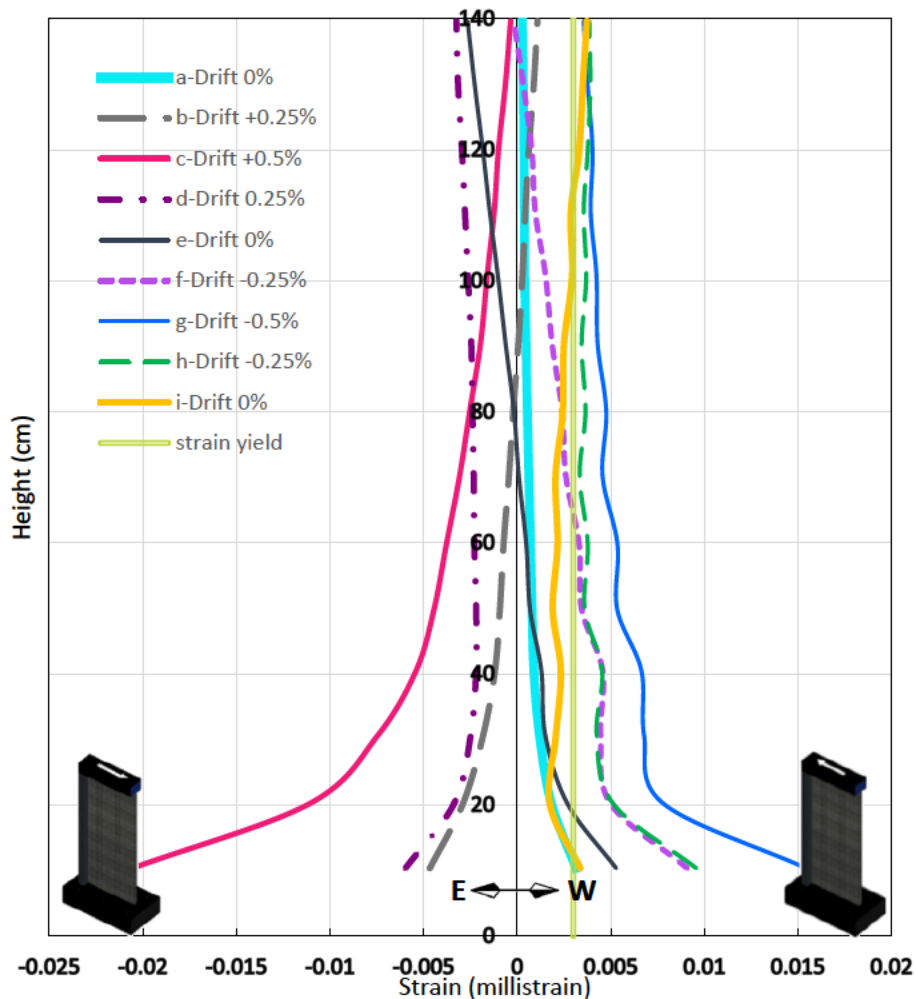
Fig. 28 Height vs. strain of the 0.5% Drift (1st cycle)
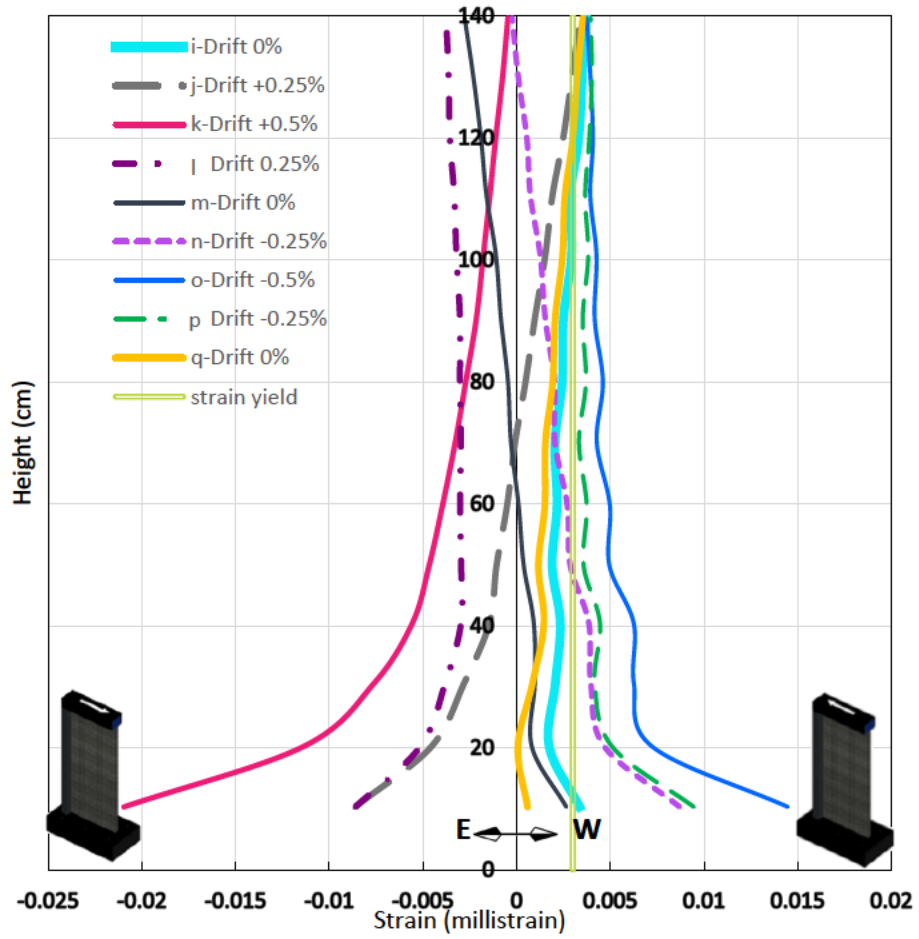
Fig. 29 Height vs. strain of the 0.5% Drift (2nd cycle)

Legend:
- a-Drift 0%
- b-Drift 0.25%
- c-Drift 0.5%
- d-Drift 0.75%
- e-Drift 0.5%
- f-Drift 0.25%
- g-Drift 0%
- h-Drift -0.25%
- i-Drift -0.5%
- j-Drift -0.75%
- k-Drift -0.5%
- l-Drift -0.25%
- m-Drift 0%
- strain yield

Y-axis: Height (cm)
X-axis: Strain (millistrain)
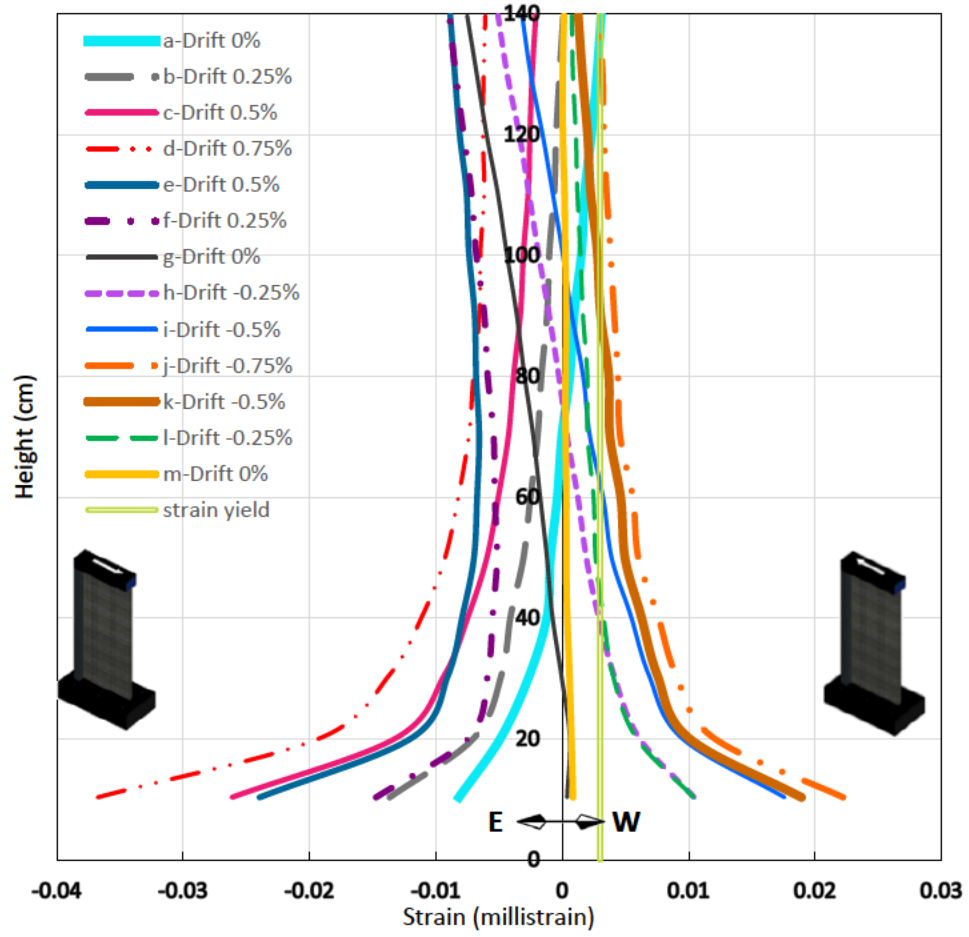
E ← → W

Fig. 30 Height vs. strain of the 0.75% Drift (1st cycle)

41
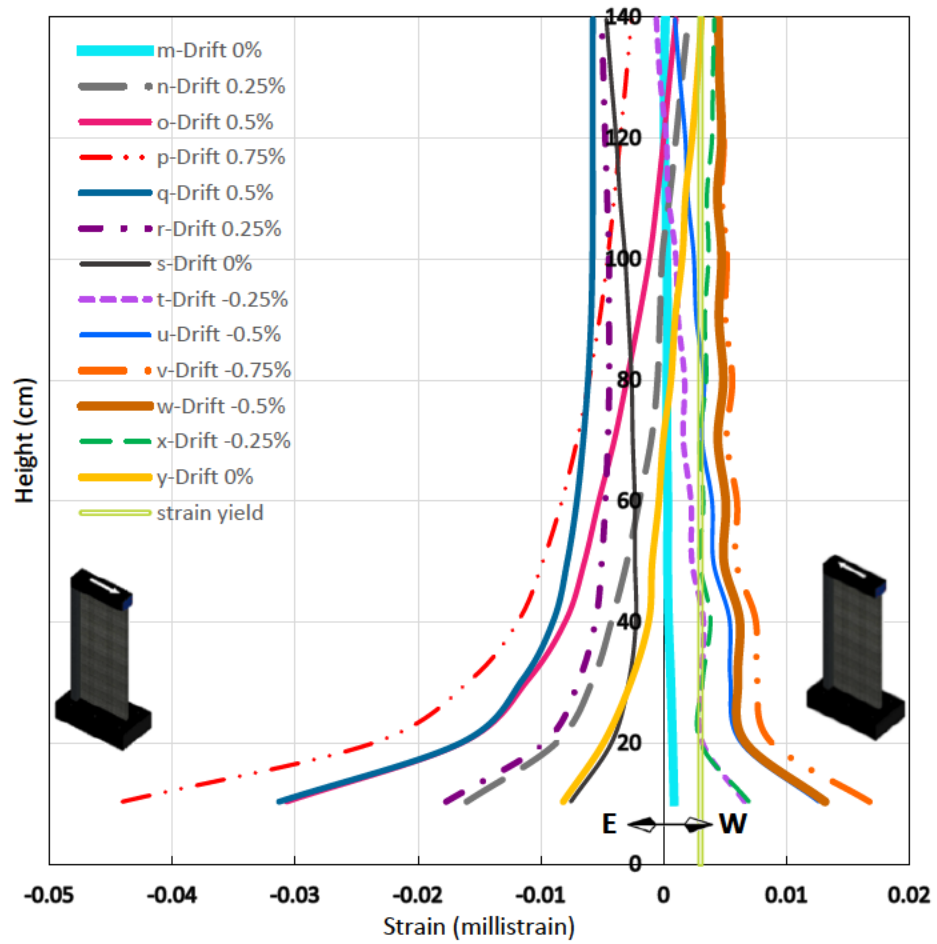
Fig. 31 Height vs. strain of the 0.75% Drift (2nd cycle)

42

Fig. 32 Strain readings between targets at the web edge

Positive drift implies that the wall was moving towards the East where the web was in compression. Whereas, negative drift implies that the wall was moving towards the West when the web was in tension. It can be concluded that the plasticity spread is going very high. The strain yield, which is equal to 3 millistrain, was reached over a height of 140 cm in the 0.5% drift and 0.75% drift.

In addition, negative strains are higher than positive strains because the forces applied to the wall during the compression cycles are higher than those applied during the tension cycles. Therefore, the displacements are going to be higher and the computed strains are going to be higher as well. And these applied forces increase with the increase of drift which lead to the increase of strain values during the compression cycles. For example, when comparing the two drifts during the second cycle, it is shown that when loading the

web in tension, the drifts are almost the same. However, when loading the web in compression, the drifts in the 0.75% drift are higher than those in the 0.5% drift.

CHAPTER FIVE

CONCLUSION AND

RECOMMENDATIONS

Studying the behavior of existing poorly designed and poorly detailed shear walls is an important task for reducing the destruction and enhancing the stability and safety of the structures when seismic events occur. The test specimens were two T-shaped slender shear walls chosen to simulate the walls present in old buildings in Lebanon, specifically in the Beirut area. This study investigated the effectiveness of a retrofit scheme that involved wrapping the wall boundary element at the web edge with a single horizontal layer of carbon fiber-reinforced polymers. The aim was to provide the necessary confinement to preserve the concrete core and prevent the buckling of the longitudinal steel bars without increasing the shear and flexure strength of the wall and retaining a ductile mode of failure. The study also evaluated the performance of existing slender shear walls, which have a single layer of reinforcement and thus no special boundary elements configuration, when subjected to in-plane cyclic loading.

The following findings can be drawn from the experimental results:

- The as-built wall specimen failed in flexure buckling. The failure mode consisted of the separation at the wall-foundation interface and buckling of the longitudinal steel bars in the web region after the crushing of the concrete.

- The retrofit of the wall specimen using CFRP sheets was effective in stabilizing the end region by providing confinement and preventing buckling failure under cyclic loading.

- In the retrofitted wall specimen, separation at the wall-foundation interface was noticed, but without any concrete crushing. However, the first three longitudinal bars in the web were fractured and the fourth one buckled.

- Compared to the as-built wall, the retrofitted wall was able to maintain its strength for a longer period. However, it did not gain much deformation capacity as it started losing strength when the reinforcing bars fractured due to fatigue in the steel.

The findings of this study conform to previous studies while presenting a better way of correcting structural deficiencies in slender shear walls that lead to considerable damage during seismic events. The experimental results are useful in demonstrating the effectiveness of fortifying slender shear walls using carbon fiber-reinforced polymer laminates. Therefore, the used process can be utilized to retrofit existing strength deficient shear walls in order to prevent or delay their collapse and reduce the threat to residents' lives when an earthquake occurs.

In any study, the acquired results are affected by the limitations and restrictions on the research plan. That is why researchers are performing more studies to address the questions that are left unanswered. The following topics develop a deeper understanding of the performance of slender shear walls under cyclic loading:

- Conducting cyclic loading tests on slender shear walls with a different layout of CFRP sheets in order to provide another set of data to compare with. Therefore, the most efficient retrofit scheme and design guidelines can be concluded.

- Performing a continuation of this study by adding axial loading to in-plane loading (the case in existing structures).

- Conducting cyclic loading tests on shear wall specimens where the drift capacity is increased to reach a capacity that is above 12.5cm.

- Emphasizing more research on the matter of fatigue in steel bars, an equally important property to yield and ultimate strength, and can have an impact on structures safety in the case of cyclic loading.

REFERENCES

Abdullah, S., and Wallace, J. (2019). Drift Capacity of Reinforced Concrete Structural Walls with Special Boundary Elements. ACI Structural Journal. 116(1), 183-194.

Chai, Y.H., and Elayer, D.T. (1999). Lateral Stability of Reinforced Concrete Columns under Axial Reversed Cyclic Tension and Compression. ACI Structural Journal. 96(5), 780-790.

Dyngeland, T. (1998). Retrofitting of bridges and building structures – a literature survey. European Laboratory for Structural Assessment, JRC-ISIS, Special Publication No. I.98.33, Ispra, 19p.

Ghosh, K.K., and Sheikh, S.A. (2007). Seismic Upgrade with Carbon Fiber-Reinforced Polymer of Columns Containing Lap-Spliced Reinforcing Bars. ACI Structural Journal. 104(2), 227–236.

Goodsir, W.J. (1985). The Design of Coupled Frame-Wall Structures for Seismic Actions [Doctoral dissertation, University of Canterbury]. UC Research Repository. http://hdl.handle.net/10092/7751

Greifenhagen, C., Lestuzzi, P. (2005). Static Cyclic Tests on Lightly Reinforced Concrete Shear Walls. Engineering Structures. 27(11), 1703-1712. https://doi.org/10.1016/j.engstruct.2005.06.008

Kaiser, H.P. (1989). Strengthening of Reinforced Concrete with Epoxy-Bonded Carbon-Fiber Plastics. Doctoral Thesis, Diss. ETH.

Khalil, A., and Ghobarah, A. (2005). Behaviour of Rehabilitated Structural Walls. Journal of Earthquake Engineering. 9(3), 371-391. doi:10.1080/13632460509350547

Kim, I., Jirsa, J.O., & Bayrak, O. (2011). Use of Carbon Fiber-Reinforced Polymer Anchors to Repair and Strengthen Lap Splices of Reinforced Concrete Columns. ACI Structural Journal. 108(5), 630–640.

Kolozvari, K., Orakcal, K., Tran, T., & Wallace, J. (2015). Modeling of Cyclic Shear-Flexure Interaction in Reinforced Concrete Structural Walls. II: Experimental

Validation.   Journal   of   Structural   Engineering.   141(5).
doi:10.1061/(ASCE)ST.1943-541X.0001083

Ladner, M., Pralong, J., & Weder, C. (1990). Geklebte Bewehrung: Bemessung und Erfahrungen. na.

Layssi, H., Cook, W.P. & Mitchell, D. (2012). Seismic Response and CFRP Retrofit of Poorly Detailed Shear Walls. Journal of Composite for Construction. 16(3), 332-339. doi:10.1061/(ASCE)CC.1943-5614.0000259

Meier, U. (1987). Bridge Repair with High Performance Composite Materials. Mater Technik. 125-128.

Meier, U., Deuring, M., Meier, H. & Schwegier, G. 1992. Strengthening of Structures with Advanced Composites. Alternative Materials for the Reinforcement and Prestressing of Concrete. 153-171.

Meier, U. (1995). Strengthening of Structures Using Carbon Fibre/Epoxy Composites. Construction and Building Materials. 9(6), 341-351. https://doi.org/10.1016/0950-0618(95)00071-2.

Parra, P.F., and Moehle, J.P. (2017). Stability of Slender Wall Boundaries Subjected to Earthquake Loading. ACI Structural Journal. 114(6), 1627-1636.

Paterson, J., and Mitchell, D. (2003). Seismic Retrofit of Shear Walls with Headed Bars and Carbon Fiber Wrap. Journal of Structural Engineering. 129(5), 606–614. doi:10.1061/(ASCE)0733-9445(2003)129:5(606)

Paulay, T., and Priestley, M.J.N. (1992). Seismic Design of Reinforced Concrete and Masonry Buildings. Wiley, New York.

Paulay, T., and Priestley, M.J.N. (1993). Stability of Ductile Structural Walls. ACI Structural Journal. 90(4), 385-392.

Priestley, M.J., Verma, R.R., & Xiao, Y. (1994). Seismic Shear Strength of Reinforced Concrete Columns. Journal of Structural Engineering. 120(8), 2310-2329. https://doi.org/10.1061/(ASCE)0733-9445(1994)120:8(2310)

Rosso, A., Almeida, J.P., & Beyer, K. (2016). Stability of Thin Reinforced Concrete Walls under Cyclic Loads: State-of-the-Art and New Experimental Findings. Bulletin of Earthquake Engineering. 14(2), 455-484. doi:10.1007/s10518-015-9827-x

Salameh, C., Guillier, B., Harb, J., Cornou, C., Bard, P. Y., Voisin, C., & Mariscal, A. (2016). Seismic response of Beirut (Lebanon) buildings: instrumental results from ambient vibrations. Bulletin of Earthquake Engineering, 14(10), 2705-2730.

Segura, C., and Wallace, J. (2018). Seismic Performance Limitations and Detailing of Slender Reinforced Concrete Walls. ACI Structural Journal. 115(3), 849-859. doi:10.14359/51701918.

Telleen, K., Maffei, J., Heintz, J., & Dragovich, J. (2012). Practical Lessons for Concrete Wall Design, Based on Studies of the 2010 Chile Earthquake.

Wallace, J. W., Massone, L. M., Bonelli, P., Dragovich, J., Lagos, R., Lüders, C., & Moehle, J. (2012). Damage and Implications for Seismic Design of RC Structural Wall Buildings. Earthquake Spectra. 28(1_suppl1), 281–299. https://doi.org/10.1193/1.4000047